Commun. Comput. Phys.
doi: 10.4208/cicp.2009.09.023

Vol. **7**, No. 1, pp. 1-46
January 2010

REVIEW ARTICLE

Local Discontinuous Galerkin Methods for High-Order Time-Dependent Partial Differential Equations

Yan Xu[1] and Chi-Wang Shu[2,*]

[1] *Department of Mathematics, University of Science and Technology of China, Hefei, Anhui 230026, China.*
[2] *Division of Applied Mathematics, Brown University, Providence, RI 02912, USA.*

Received 29 January 2009; Accepted (in revised version) 22 May 2009

Available online 3 June 2009

Abstract. Discontinuous Galerkin (DG) methods are a class of finite element methods using discontinuous basis functions, which are usually chosen as piecewise polynomials. Since the basis functions can be discontinuous, these methods have the flexibility which is not shared by typical finite element methods, such as the allowance of arbitrary triangulation with hanging nodes, less restriction in changing the polynomial degrees in each element independent of that in the neighbors (p adaptivity), and local data structure and the resulting high parallel efficiency. In this paper, we give a general review of the local DG (LDG) methods for solving high-order time-dependent partial differential equations (PDEs). The important ingredient of the design of LDG schemes, namely the adequate choice of numerical fluxes, is highlighted. Some of the applications of the LDG methods for high-order time-dependent PDEs are also be discussed.

AMS subject classifications: 65M60

Key words: Discontinuous Galerkin method, local discontinuous Galerkin method, numerical flux, stability, time discretization, high order accuracy, stability, error estimates.

Contents

*Corresponding author. *Email addresses:* yxu@ustc.edu.cn (Y. Xu), shu@dam.brown.edu (C.-W. Shu)

1 Overview

1.1 Brief introduction of the discontinuous Galerkin method

The discontinuous Galerkin (DG) method that we discuss in this paper is a class of finite element methods using a discontinuous piecewise polynomial space for the numerical solution and the test functions in the spatial variables, coupled with explicit or implicit nonlinearly stable high order time discretization. These methods have found their way into the main stream of computational fluid dynamics and other areas of applications.

The first DG method was introduced in 1973 by Reed and Hill [77], in the framework of neutron transport, i.e. a time independent linear hyperbolic equation. It was later developed for solving nonlinear hyperbolic conservation laws with first derivatives by Cockburn et al. in a series of papers [29,35,37,39], in which they have established a framework to easily solve nonlinear time dependent problems, such as the Euler equations in compressible gas dynamics, using explicit, nonlinearly stable high order Runge-Kutta time discretizations [85] and DG discretization in space with exact or approximate Riemann solvers as interface fluxes and total variation bounded (TVB) nonlinear limiters [82] to achieve non-oscillatory properties for strong shocks.

Since the basis functions can be discontinuous, the DG methods have certain flexibility and advantage, such as,

- It can be easily designed for any order of accuracy. In fact, the order of accuracy can be locally determined in each cell.
- It is easy to handle complicated geometry and boundary conditions. It can be used on arbitrary triangulations, even those with hanging nodes.
- It is local in data communications. The evolution of the solution in each cell needs to communicate only with its immediate neighbors, regardless of the order of accuracy. The methods have high parallel efficiency, usually more than 99% for a fixed mesh, and more than 80% for a dynamic load balancing with adaptive meshes which change often during time evolution, see, e.g. [12,78].
- There is provable cell entropy inequality and L^2 stability, for arbitrary scalar equations in any spatial dimension and any triangulation, for any order of accuracy, without limiters [60].
- It is at least $(k+\frac{1}{2})$-th order accurate, and often $(k+1)$-th order accurate in L^2 norm for smooth solutions when piecewise polynomials of degree k are used, regardless of the structure of the meshes.
- It is flexible to *h-p* adaptivity. A very good example to illustrate the capability of the DG method in *h-p* adaptivity, efficiency in parallel dynamic load balancing, and

good resolution properties is the successful simulation of the Rayleigh-Taylor flow instabilities in [78].

The DG method has found rapid applications in such diverse areas as aeroacoustics, electro-magnetism, gas dynamics, granular flows, magneto-hydrodynamics, meteorology, modeling of shallow water, oceanography, oil recovery simulation, semiconductor device simulation, transport of contaminant in porous media, turbomachinery, turbulent flows, viscoelastic flows and weather forecasting, among many others. For a detailed description of the method as well as its implementation and applications, we refer to the lecture notes [26, 84], the survey paper [34], and other papers in that Springer volume, which contains the conference proceedings of the First International Symposium on DG Methods held at Newport, Rhode Island in 1999. The extensive review paper [40] is also a good reference for many details. More recently, there are at least four books [58,63,68,79] covering different aspects of the DG method. There are also three special journal issues [41,42,46] devoted to the DG method, which contain many interesting papers in the development of the method in all aspects including algorithm design, analysis, implementation and applications.

1.2 Development of the DG method for high order partial differential equations

In this paper we mainly discuss a class of DG methods for solving time dependent partial differential equations (PDEs) with higher derivatives, which are termed local DG (LDG) methods. The idea of LDG methods is to suitably rewrite a higher order PDE into a first order system, then apply the DG method to the system. A key ingredient for the success of such methods is the correct design of interface numerical fluxes. These fluxes must be designed to guarantee stability and local solvability of all the auxiliary variables introduced to approximate the derivatives of the solution.

The first LDG method was designed to solve a convection diffusion equation (with second derivatives) by Cockburn and Shu [38]. Their work was motivated by the successful numerical experiments of Bassi and Rebay [10] for the compressible Navier-Stokes equations. The LDG method is in the same form as the general DG spatial discretization used for purely convective non-linear systems, with a different guiding principle for the choice of the numerical fluxes. Of course, it is efficient to use explicit Runge-Kutta time discretizations for convection diffusion problems only if the convection is actually dominant. We briefly discuss the issue of time discretization in Section 6. Later, Yan and Shu developed a LDG method for a general KdV type equation with third order derivatives in [104], and they generalized the LDG method to PDEs with fourth and fifth spatial derivatives in [105]. Levy, Shu and Yan [67] developed LDG methods for nonlinear dispersive equations that have compactly supported traveling wave solutions, the so-called "compactons". More recently, Eskilsson and Sherwin [50–52] presented discontinuous spectral element methods for simulating 1D linear Boussinesq-type equations, dispersive shallow water systems and 2D Boussinesq equations. Xu and Shu further generalized the

LDG method to solve a series of nonlinear wave equations [96–99]. LDG methods have been generalized to transport equations [4, 47], three-dimensional shallow water flow [3] and Richards' equation [69, 70]. There is also recent work in developing LDG methods for the model problems in phase transition [57], porous medium equation [90, 109] and singularly perturbed problems [95].

There is a lot of recent research on LDG discretizations for second order elliptic equations. Recent development and analysis of the LDG methods for elliptic equations can be found in, e.g., [19–22, 24, 44, 45]. LDG methods for the Stokes system were introduced in [33]. The LDG methods for linearized incompressible fluid flow were presented and reviewed in [30–32, 81]. The minimal dissipation LDG method for convection-diffusion or diffusion problems was analyzed in [27]. In [13] Burman and Stamm considered the minimal stabilization to the case of the LDG methods in a mixed form. Preconditioning techniques for solving the linear system of LDG method were considered in [23, 61, 62]. Bustinza and Gatica presented and analyzed a LDG method for a class of nonlinear diffusion problems with mixed boundary conditions in [15, 16]. The residual-based reliable a posteriori error estimate for the LDG approximations of linear and nonlinear diffusion problems in polygonal regions was proved in [17]. Later, Bustinza analyzed the main features of the LDG method applied to nonlinear boundary value problems in the plane [14]. More recently, the coupling of LDG and boundary element methods was considered to solve a class of non-linear exterior transmission problems in the plane [18].

The LDG method can retain the flexibility of the DG method since the auxiliary variables can be locally eliminated. However, practitioners are sometimes unhappy with these auxiliary variables, since they may increase the complexity and computational cost of the method, and they expand the effective stencil of the method after the elimination of the auxiliary variables. An alternative method for solving second order convection diffusion equations is the DG method of Baumann and Oden [11], see also [75]. This method does not need the introduction of auxiliary variables, relying instead on penalty terms at cell boundaries to achieve stability. However, this method does not achieve the optimal $(k+1)$-th order of accuracy in L^2 norm when piecewise polynomials of degree k is used (this accuracy degeneracy is well known for even k and is also shown to exist for odd k recently in [56]). Also, it does not seem straight-forward to generalize this method to nonlinear PDEs with higher order spatial derivatives. Another class of related methods, mostly for elliptic problems with even-order leading derivatives and without time, is the class of interior penalty (IP) methods, see for example Baker [9], and also [6, 7]. The IP methods use penalty terms, which are typically proportional to the jumps of the solution and are added to all interior cell interfaces for stability.

More recently, van Leer and Nomura [88] (see also van Raalte and van Leer [89]) and Gassner *et al*. [54] proposed new DG formulations for the diffusion equations. They use twice the integration by parts for the diffusion term, and either an L^2 projection of the discontinuous piecewise polynomial over two neighboring cells into a continuous, single polynomial, or a suitable Riemann solver for the diffusion equation, that is, exact solutions for the diffusion equation with a step function Riemann initial data, to provide

interface values of the solution derivative resulting from the integration by parts. The DG schemes in [88] and [54] do not need to use auxiliary variables as in LDG method, however the L^2 projection procedure might be cumbersome for arbitrary triangulations in multi-dimensions, especially for non-conforming meshes with hanging nodes, while the Riemann solver based approach might be difficult to be generalized to equations with higher order spatial derivatives. In [1], Adjerid and Temimi introduced a DG method for solving high order ordinary differential equations (ODEs). Their method uses repeated integrations by parts with taking all the numerical fluxes from the left.

The method designed by Cheng and Shu in [25] also uses repeated integration by parts, and relies on suitably chosen numerical fluxes for all derivatives of the numerical solution up to one order lower than the order of the PDE. Advantages of this approach in comparison with the IP type methods include its automatic local conservation, and its ability to design stable DG methods for wave type PDEs with odd-order leading derivatives such as the KdV equations. In [25], a framework of designing DG schemes that work for general time dependent PDEs with higher order spatial derivatives were developed, by carefully choosing the numerical fluxes to ensure *provable* stability. Similar to [1, 54, 88, 89], the methods in [25] also depend on repeated integration by parts; and similar to [1], the methods also depend on the choice of numerical fluxes at the cell interfaces. However, since the PDEs contain possibly nonlinear higher order derivative terms, the simple choice of taking the numerical fluxes always from the left does not work and a carefully designed set of numerical fluxes for different PDEs to ensure stability is essential.

Another DG method for solving second order diffusion problems is introduced by Liu and Yan in [72], which the authors called the direct discontinuous Galerkin (DDG) method. Unlike the traditional LDG method, the DDG method is based on a direct weak formulation for the parabolic equation in each computational cell, and an inter-cell communication via the numerical flux $\widehat{u_x}$. A general numerical flux formula for the solution derivative is proposed. In comparison with the DG methods in [1, 25, 54, 88], which rely on repeated integration by parts for the diffusion term so that interface values can be imposed for both the solution and its derivatives, the DDG method in [72] relies on the standard weak formulation for parabolic equations with integration by parts only once, hence the numerical flux is defined only for the solution derivative, however this numerical flux depends on the jumps of *all* the derivatives of the numerical solution at the cell interface. Error estimates are provided in [72]. However, it is not clear how this method can be generalized to higher order PDEs.

1.3 Outline of the paper

In this paper, we give a general review of the LDG methods for higher order time-dependent PDEs. To set up the necessary background, the essential idea of the DG scheme for hyperbolic conservation laws is explained in Section 2. In Section 3 we describe the LDG method for the diffusion equations. We start with the simple one dimen-

sional scalar heat equation and explain the difficulty in generalizing the DG method to PDEs with higher order spatial derivatives. Then we remark on the procedure to extend the algorithm to handle nonlinearity, systems, and multi-space dimensions. Some applications are also shown. In Section 4, we generalize the LDG method to dispersive equations. Some additional topics related to the LDG method are discussed in Section 5. In Section 6, we discuss time discretization issues. Finally, in Section 7, we mention a few topics on LDG schemes for PDEs with high order derivatives.

2 The DG method for hyperbolic conservation laws

A simple example to illustrate the essential ideas of DG method is the scalar one-dimensional conservation law equation

$$u_t+f(u)_x=0, \quad x\in[a,b]. \tag{2.1}$$

Let $a=x_{\frac{1}{2}}<x_{\frac{3}{2}}<\cdots<x_{N+\frac{1}{2}}=b$ be a partition of $I=[a,b]$. We denote the mesh by $I_j=[x_{j-\frac{1}{2}},x_{j+\frac{1}{2}}]$, for $j=1,\cdots,N$. The center of the cell is $x_j=(x_{j-\frac{1}{2}}+x_{j+\frac{1}{2}})/2$ and $\Delta x_j=x_{j+\frac{1}{2}}-x_{j-\frac{1}{2}}$. To simplify the notation, we still use u to denote the numerical solution. If we multiply (2.1) by an arbitrary test function v, integrate over the interval I_j, and integrate by parts, we get the weak formulation

$$\int_{I_j}u_tvdx-\int_{I_j}f(u)v_xdx+f(u_{j+\frac{1}{2}})v_{j+\frac{1}{2}}-f(u_{j-\frac{1}{2}})v_{j-\frac{1}{2}}=0. \tag{2.2}$$

Notice that now both the solution u and the test function v are piecewise polynomials of degree at most k. We denote by $V_{\Delta x}$ the space of polynomials of degree up to k in each cell I_j, i.e.

$$V_{\Delta x}=\{v:\ v\in P^k(I_j)\ \text{ for }\ x\in I_j,\ j=1,\cdots,N\}. \tag{2.3}$$

With this choice, there is an ambiguity in (2.2) in the last two terms involving the boundary values at $x_{j+\frac{1}{2}}$, as both the solution u and the test function v are discontinuous at these boundary points. One should design these terms so that the resulting numerical method is stable and accurate. We denote $u^+_{j+\frac{1}{2}}$ and $u^-_{j+\frac{1}{2}}$ the values of u at $x_{j+\frac{1}{2}}$, from the right cell I_{j+1}, and from the left cell I_j, respectively. The boundary terms are then handled as follows.

- Replace the boundary terms $f(u_{j\pm\frac{1}{2}})$ by single valued numerical fluxes $\hat{f}_{j\pm\frac{1}{2}}=\hat{f}(u^-_{j\pm\frac{1}{2}},u^+_{j\pm\frac{1}{2}})$. These fluxes in general depend both on the left limit and on the right limit. The idea is to treat these terms by an upwinding mechanism (information from characteristics), borrowed from successful high resolution finite volume schemes. For the equation (2.1), the flux $\hat{f}_{j+\frac{1}{2}}$ is taken as a monotone numerical flux, i.e. it is Lipschitz continuous in both arguments, consistent ($\hat{f}(u,u)=f(u)$),

non-decreasing in the first argument and non-increasing in the second argument. Examples of monotone fluxes which are suitable for discontinuous Galerkin methods can be found in, e.g., [37]. We could for example use the simple Lax-Friedrichs flux

$$\hat{f}(u^-,u^+)=\frac{1}{2}(f(u^-)+f(u^+)-\alpha(u^+-u^-)),\quad \alpha=\max|f'(u)|,$$

where the maximum is taken over a relevant range of u.

- Replace the test function v at the boundaries by $v^-_{j+\frac{1}{2}}$ and $v^+_{j-\frac{1}{2}}$.

The scheme is then given by: Find $u\in V_{\Delta x}$, such that $\forall v\in V_{\Delta x}$, we have

$$\int_{I_j} u_t v dx-\int_{I_j} f(u)v_x dx+\hat{f}_{j+\frac{1}{2}}v^-_{j+\frac{1}{2}}-\hat{f}_{j-\frac{1}{2}}v^+_{j-\frac{1}{2}}=0. \tag{2.4}$$

The resulting method of the lines ODE (2.4) is then discretized by the nonlinearly stable high order Runge-Kutta time discretizations [85]. The most popular scheme in this class is the following third order Runge-Kutta method for solving

$$\dot{u}=L(u,t), \tag{2.5}$$

where $L(u,t)$ is a spatial discretization operator (it does not need to be, and often is not, linear):

$$\begin{aligned}
u^{(1)}&=u^n+\Delta tL(u^n,t^n),\\
u^{(2)}&=\frac{3}{4}u^n+\frac{1}{4}u^{(1)}+\frac{1}{4}\Delta tL(u^{(1)},t^n+\Delta t),\\
u^{n+1}&=\frac{1}{3}u^n+\frac{2}{3}u^{(2)}+\frac{2}{3}\Delta tL(u^{(2)},t^n+\frac{1}{2}\Delta t).
\end{aligned} \tag{2.6}$$

3 The LDG method for diffusion equations

In this section, we discuss the development of the LDG methods for the diffusion equations, such as heat equation, convection diffusion equations, biharmonic equation, and Cahn-Hilliard equations, etc.

3.1 Difficulty in the generalization of DG to PDEs with higher order spatial derivatives

For equations with higher order spatial derivatives, it is more difficult to design DG methods. The solution space, which consists of piecewise polynomials which are discontinuous at the element interfaces, is more unnatural for approximating higher order derivatives.

A naive generalization of the DG method to a PDE with higher spatial derivatives could have disastrous results. Consider, as a simple example, the heat equation

$$u_t - u_{xx} = 0, \tag{3.1}$$

for $x \in [0,2\pi]$ with periodic boundary conditions and with an initial condition $u(x,0) = \sin(x)$. A straightforward generalization of the DG method from the hyperbolic equation $u_t + f(u)_x = 0$ is to write down the same scheme and replace $f(u)$ by $-u_x$ everywhere. Namely, find $u \in V_{\Delta x}$ such that, for all test functions $v \in V_{\Delta x}$,

$$\int_{I_j} u_t v dx + \int_{I_j} u_x v_x dx - \widehat{u_x}_{j+\frac{1}{2}} v^-_{j+\frac{1}{2}} + \widehat{u_x}_{j-\frac{1}{2}} v^+_{j-\frac{1}{2}} = 0. \tag{3.2}$$

Lacking an upwinding consideration for the choice of the flux u_x and considering that diffusion is isotropic, a natural choice for the flux is the central flux

$$\widehat{u_x}_{j+\frac{1}{2}} = \frac{1}{2}((u_x)^+_{j+\frac{1}{2}} + (u_x)^-_{j+\frac{1}{2}}). \tag{3.3}$$

Fig. 1 [108] shows the numerical solution with 40 and 320 cells versus the exact solution, for the two cases $k = 1$ and 2 (piecewise linear and piecewise quadratic cases) at t = 0.7. This application of the DG method directly to the heat equation with second derivatives could yield a method which behaves nicely in the computation, in the sense that a grid refinement study seems to produce a numerically convergent solution, but is mathematically weakly unstable and has $\mathcal{O}(1)$ errors to the exact solution in numerical tests (hence it looks "inconsistent") [40, 83, 108].

A DG method which was designed in [10, 38] is to first rewrite the equation (3.1) into a first order system

$$u_t - q_x = 0, \qquad q - u_x = 0, \tag{3.4}$$

then formally use the same DG method for the convection equation to solve (3.4), resulting in the following scheme: Find $u, q \in V_{\Delta x}$, $\forall v, w \in V_{\Delta x}$, such that

$$\begin{aligned} &\int_{I_j} u_t v dx + \int_{I_j} q v_x dx - \hat{q}_{j+\frac{1}{2}} v^-_{j+\frac{1}{2}} + \hat{q}_{j-\frac{1}{2}} v^+_{j-\frac{1}{2}} = 0, \\ &\int_{I_j} q w dx + \int_{I_j} u w_x dx - \hat{u}_{j+\frac{1}{2}} w^-_{j+\frac{1}{2}} + \hat{u}_{j-\frac{1}{2}} w^+_{j-\frac{1}{2}} = 0. \end{aligned} \tag{3.5}$$

However, there is no longer a upwinding mechanism or characteristics to guide the design of the fluxes $\hat{u}_{j+\frac{1}{2}}$ and $\hat{q}_{j+\frac{1}{2}}$. The crucial part in designing a stable and accurate algorithm (3.5) is a correct design of these fluxes. In [38], criteria are given for these fluxes to guarantee stability, convergence and a sub-optimal error estimate of order k in L^2 norm for piecewise polynomials of degree k. The (most natural) central fluxes

$$\hat{u}_{j+\frac{1}{2}} = \frac{1}{2}(u^+_{j+\frac{1}{2}} + u^-_{j+\frac{1}{2}}), \quad \hat{q}_{j+\frac{1}{2}} = \frac{1}{2}(q^+_{j+\frac{1}{2}} + q^-_{j+\frac{1}{2}}) \tag{3.6}$$

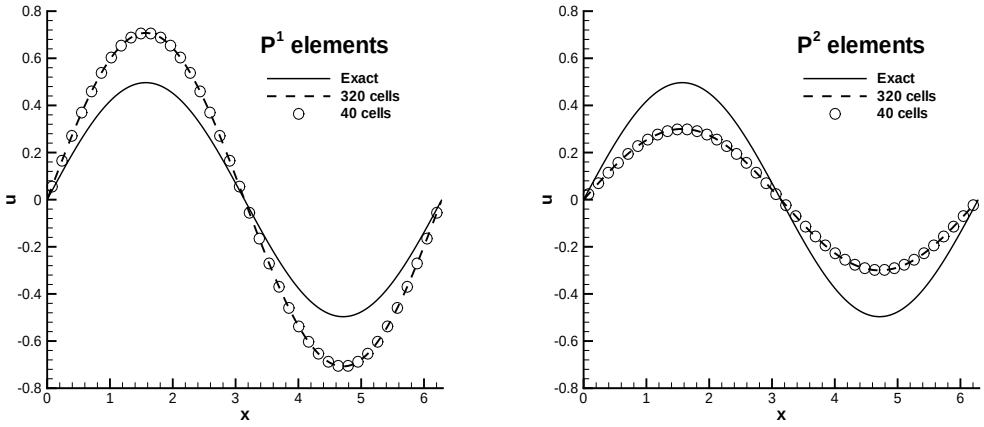

Figure 1: Reproduced from [108]. The "inconsistent" discontinuous Galerkin method (3.2) applied to the heat equation (3.1) with an initial condition $u(x;0)=\sin(x)$. t = 0.7. 160 cells. Third order Runge-Kutta in time. Solid line: the exact solution; Dashed line and squares symbols: the computed solution at the cell centers. Left: $k=1$; Right: $k=2$.

would satisfy these criteria and give a scheme which is indeed sub-optimal in L^2 norm in the order of accuracy for odd k (i.e. the accuracy is order k rather than the expected order $k+1$ in L^2 norm for odd k). This deficiency, however, can be removed by adopting another choice of fluxes as proposed in [38]

$$\hat{u}_{j+\frac{1}{2}}=u^+_{j+\frac{1}{2}},\quad \hat{q}_{j+\frac{1}{2}}=q^-_{j+\frac{1}{2}}, \tag{3.7}$$

i.e. we alternatively take the left and right limits for the fluxes in u and q (we could of course also take the pair $u^-_{j+\frac{1}{2}}$ and $q^+_{j+\frac{1}{2}}$ as the fluxes). Notice that the evaluation of (3.7) is simpler than that of the central fluxes in (3.6), and this easily generalizes to multi space dimensions on arbitrary triangulations. The accuracy now becomes the optimal order $k+1$ in L^2 norm for both even and odd k. The appearance of the auxiliary variable q is superficial: when a local basis is chosen in cell I_j then q is eliminated by the second equation in (3.5) with the inversion of a small mass matrix. To be more specific, the second equation in (3.5) would give us $q=Bu$ for a block banded matrix B, which can be substituted into the first equation in (3.5) to obtain a scheme (ODE) for u which takes a similar form as that for the convection equation. This is a big advantage of the scheme over the traditional "mixed methods", and it is the reason that the scheme is termed LDG method in [38]. Even though the auxiliary variable q can be locally eliminated, it does approximate the derivative of the solution u to the same order of accuracy, thus matching the advantage of the traditional "mixed methods" that the solution and its derivative are approximated to the same order of accuracy.

For illustration purpose we show in Table 1 [108] the L^2 and L^∞ errors and numerically observed orders of accuracy, for both u and q, for the two cases $k=1$ and 2 (piece-

Table 1: Reproduced from [108]. L^2 and L^∞ errors and orders of accuracy for the LDG method (3.5) with fluxes (3.7) applied to the heat equation (3.1) with an initial condition $u(x,0)=\sin(x)$, $t=1$. Third order Runge-Kutta in time with a small Δt so that time error can be ignored.

	$k=1$				$k=2$			
Δx	L^2 error	order	L^∞ error	order	L^2 error	order	L^∞ error	order
$2\pi/20, u$	1.58E-03	—	6.01E-03	—	3.98E-05	—	1.89E-04	—
$2\pi/20, q$	1.58E-03	—	6.01E-03	—	3.98E-05	—	1.88E-04	—
$2\pi/40, u$	3.93E-04	2.00	1.51E-03	1.99	4.98E-06	3.00	2.37E-05	2.99
$2\pi/40, q$	3.94E-04	2.00	1.51E-03	1.99	4.98E-06	3.00	2.37E-05	2.99
$2\pi/80, u$	9.83E-05	2.00	3.78E-04	2.00	6.22E-07	3.00	2.97E-06	3.00
$2\pi/80, q$	9.83E-05	2.00	3.78E-04	2.00	6.22E-07	3.00	2.97E-06	3.00
$2\pi/160, u$	2.46E-05	2.00	9.45E-05	2.00	7.78E-08	3.00	3.71E-07	3.00
$2\pi/160, q$	2.46E-05	2.00	9.45E-05	2.00	7.78E-08	3.00	3.71E-07	3.00

wise linear and piecewise quadratic cases) to $t=1$. Clearly $(k+1)$-th order of accuracy is achieved for both odd and even k and also the same order of accuracy is achieved for q which approximates u_x. We thus obtain the advantage of mixed finite element methods in approximating the derivatives of the exact solution to the same order of accuracy as the solution themselves, yet without additional storage or computational costs for the auxiliary variable q.

3.2 The LDG method for the convection diffusion equations

In the following we discuss the LDG method for the convection diffusion equations in [38]

$$u_t+\sum_{i=1}^{d} f_i(u)_{x_i}-\sum_{i=1}^{d}\sum_{j=1}^{d}(a_{ij}(u)u_{x_j})_{x_i}=0, \quad d\geq 1, \tag{3.8}$$

with an initial condition

$$u(x_1,\cdots,x_d,0)=u_0(x_1,\cdots,x_d), \tag{3.9}$$

and periodic boundary conditions, where $f_i(u)$ and $a_{ij}(u)$ are arbitrary (smooth) nonlinear functions and $a_{ij}(u)$ are entries of a symmetric and semi-positive definite matrix. A symmetric and semi-positive definite matrix has a square root, i.e. there exists a symmetric and semi-positive definite matrix $b_{ij}(u)$ such that

$$a_{ij}(u)=\sum_{1\leq l\leq d} b_{il}(u)b_{lj}(u), \tag{3.10}$$

and we denote

$$g_{lj}(u)=\int^u b_{lj}(\tau)d\tau. \tag{3.11}$$

To define the LDG method, we rewrite the equation (3.8) as a first order system:

$$u_t+\sum_{i=1}^{d}f_i(u)_{x_i}-\sum_{i=1}^{d}\Big(\sum_{l=1}^{d}b_{il}(u)q_l\Big)_{x_i}=0, \tag{3.12a}$$

$$q_l-\sum_{j=1}^{d}(g_{lj}(u))_{x_j}=0,\quad l=1,\cdots,d. \tag{3.12b}$$

Notice that the usage of the square root matrix (3.10) helps the analysis, however in practical computation people often ignore it and define the auxiliary variable simply as $q_l=u_{x_l}$. For an arbitrary triangulation, let $\mathbb{T}_h$ denote a tessellation of Ω with shape-regular elements K. Let Γ denote the union of the boundary faces of elements $K\in\mathbb{T}_h$, i.e. $\Gamma=\cup_{K\in\mathbb{T}_h}\partial K$, and $\Gamma_0=\Gamma\backslash\partial\Omega$. Let $P^k(K)$ be the space of polynomials of degree at most $k\geq 0$ on $K\in\mathbb{T}_h$. We denote the finite element space by

$$W_h=\{v:\ v|_K\in P^k(K)\ \text{ for }\ \forall K\in\mathbb{T}_h\}. \tag{3.13}$$

In order to describe the flux functions we need to introduce some notations. We choose a fixed vector $\boldsymbol{\beta}$ which is not parallel with any normals of element boundaries. This is possible because there are only finitely many element boundary normals for any given mesh, including meshes with possible curved edges since we are concerned only with the normals at the quadrature points along element edges. For example, we can choose $\boldsymbol{\beta}=(1,1)$ for the rectangular mesh. For each face e, we use this fixed vector $\boldsymbol{\beta}$ to uniquely define the "left" and "right" elements K_L and K_R which share the same face e. The "right" side is the side at the end of the arrow of the normal $\boldsymbol{n}$ with $\boldsymbol{n}\cdot\boldsymbol{\beta}>0$ and the "left" side is naturally the opposite side. See Fig. 2 for an illustration. If ψ is a function on K_L and K_R, but possibly discontinuous across e, let ψ_L denote $(\psi|_{K_L})|_e$ and ψ_R denote $(\psi|_{K_R})|_e$, the left and right trace, respectively.

Now we can use the LDG method to approximate Eq. (3.12). Find u, $q_1,\cdots,q_d\in W_{\Delta x}$, such that, $\forall\rho$, $\psi_1,\cdots,\psi_d\in W_{\Delta x}$,

$$\begin{aligned}&\int_K(u_h)_t\rho dx-\sum_{i=1}^{d}\int_K f_i(u)\rho_{x_i}dx+\sum_{i=1}^{d}\int_K(\sum_{l=1}^{d}b_{il}(u)q_l)\rho_{x_i}dx\\&\quad+\int_{\partial K}\widehat{f}(u^L,u^R,\mathbf{n})\rho ds-\sum_{i=1}^{d}\int_{\partial K}\Big(\sum_{l=1}^{d}\widehat{b_{il}(u)}\widehat{q_l}n_i\Big)\rho ds=0,\end{aligned} \tag{3.14a}$$

$$\int_K q_l\psi_l dx+\sum_{j=1}^{d}\int_K g_{lj}(u)(\psi_l)_{x_j}dx-\sum_{j=1}^{d}\int_{\partial K}\widehat{g_{lj}(u)}n_j\psi_l ds=0,\quad l=1,\cdots,d, \tag{3.14b}$$

where $\mathbf{n}=(n_1,\cdots,n_d)$ denotes the outward unit normal to the element K at $x\in\partial K$. The "hat" terms in (3.14) are the numerical fluxes. It turns out that we can take the simple choices such that

$$\widehat{b_{il}(u)}=\frac{g_{il}(u^R)-g_{il}(u^L)}{u^R-u^L},\quad \widehat{g_{lj}(u)}=g_{lj}(u^L),\quad \widehat{q_l}=q_l^R, \tag{3.15}$$

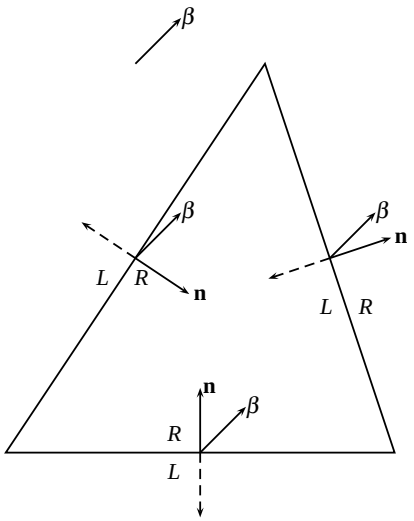

Figure 2: Illustration of the definition of "right" and "left" sides determined by a pre-determined vector β.

and $\widehat{f}(u^L,u^R,\mathbf{n})$ is any one-dimensional monotone flux which is conservative and consistent with the nonlinearity $\sum_{i=1}^{d} f_i(u)n_i$. Now the algorithm is well defined.

Remark 3.1. Choice for the numerical fluxes
The numerical fluxes at the boundary terms should be designed based on different guiding principles for different PDEs to ensure stability. For example, upwinding should be used as a guideline for odd derivatives which correspond to waves, and symmetric treatment, such as an alternating choice of the fluxes for a quantity and its derivative, should be used for even derivatives.

Remark 3.2. L^2 **stability**
For the scheme (3.14) with the numerical fluxes (3.15), we have the following result on cell entropy inequality [38]:

Proposition 3.1 (cell entropy inequality)**.** *There exist conservative numerical entropy fluxes* $\widehat{\Psi_{\mathbf{n}_K,K}}$ *such that the solution to the scheme* (3.14)-(3.15) *satisfies*

$$\frac{d}{dt}\int_K \left(\frac{u^2(x,t)}{2}\right)dx+\int_{\partial K}\widehat{\Psi_{\mathbf{n}_K,K}}ds\leq 0. \tag{3.16}$$

Here "conservative" fluxes refer to the fact that $\widehat{\Psi_{\mathbf{n}_K,K}}=-\widehat{\Psi_{\mathbf{n}'_{K'},K'}}$ *on the edge shared by the two elements* K *and* K'.

The L^2 stability of the method is then a trivial corollary, by summing up the cell entropy inequalities over K and assuming periodic boundary conditions [38]:

Corollary 3.1 (L^2 stability)**.** *The solution to the scheme* (3.14)-(3.15) *satisfies the* L^2 *stability*

$$\frac{d}{dt}\int_\Omega \left(\frac{u^2(x,t)}{2}\right)dx \leq 0. \tag{3.17}$$

The cell entropy inequality and L^2 stability can be proved in any spatial dimension and any triangulation, for any order of accuracy. Such results are typical for LDG methods for various nonlinear PDEs with higher order spatial derivatives.

Remark 3.3. Error estimates
The optimal $\mathcal{O}(h^{k+1})$ error estimates in L^2 norm can be obtained on tensor product meshes and polynomial spaces for the smooth solution of Eq. (3.8). For general triangulations and piecewise polynomials of degree k, a sub-optimal error estimate of $\mathcal{O}(h^k)$ in L^2 norm can be obtained [38, 100].

3.3 Applications of the LDG method for other diffusion equations

3.3.1 Bi-harmonic equations

An LDG scheme for solving the time dependent convection bi-harmonic equation

$$u_t + \sum_{i=1}^{d} f_i(u)_{x_i} + \sum_{i=1}^{d} (a_i(u_{x_i})u_{x_i x_i})_{x_i x_i} = 0, \tag{3.18}$$

where $f_i(u)$ and $a_i(q) \geq 0$ are arbitrary functions, was designed in [105]. The numerical fluxes are chosen following the same "alternating fluxes" principle similar to the second order convection diffusion equation (3.8), see (3.15). A cell entropy inequality and the L^2 stability of the LDG scheme for the nonlinear equation (3.18) can be proved [105], which do not depend on the smoothness of the solution of (3.18), the order of accuracy of the scheme, or the triangulation. In [48], optimal error estimates in L^2 norm were obtained for fourth-order linear biharmonic equations in one and multi-dimensions for both Cartesian and triangular meshes. The analysis in [48] can also be extended to higher even-order equations and the linearized Cahn-Hilliard type equations.

We show the results of the linear bi-harmonic equation (3.18) in [105]:

$$u_t + u_{xxxx} = 0, \tag{3.19}$$

with initial condition $u(x,0) = \sin(x)$ and periodic boundary conditions. The exact solution is given by $u(x,t) = e^{-t}\sin(x)$. The numerical errors and order of accuracy can be found in Table 2. We clearly observe an accuracy of Δx^{k+1} when piecewise P^k elements are used.

Table 2: Reproduced from [105]. $u_t+u_{xxxx}=0$. $u(x,0)=\sin(x)$. Periodic boundary conditions. L^∞ errors. Uniform meshes with N cells. LDG methods with $k=0,1,2,3$. $t=1$.

k	N=10	N=20		N=40		N=80	
	error	error	order	error	order	error	order
0	1.1125E-01	5.4352E-02	1.03	2.7001E-02	1.00	1.3478E-02	1.00
1	2.2038E-02	5.2262E-03	2.07	1.3119E-03	1.99	3.2831E-04	1.99
2	1.1183E-03	1.3512E-04	3.04	1.6988E-05	2.99	2.1265E-06	2.99
3	6.1004E-05	2.3484E-06	4.69	1.4022E-07	4.06	8.7476E-09	4.00

3.3.2 The Kuramoto-Sivashinsky type equations

In [99], an LDG method has been developed to solve the Kuramoto-Sivashinsky type equations

$$u_t+f(u)_x-(a(u)u_x)_x+(r'(u)g(r(u)_x)_x)_x+(s(u_x)u_{xx})_{xx}=0, \tag{3.20}$$

where $f(u)$, $a(u)\geq 0$, $r(u)$, $s(p)\geq 0$ and $g(p)$ are arbitrary (smooth) nonlinear functions. The Kuramoto-Sivashinsky equation

$$u_t+uu_x+\alpha u_{xx}+\beta u_{xxxx}=0, \tag{3.21}$$

where α and β are constants. The Kuramoto-Sivashinsky equation, a special case of (3.20), is a canonical evolution equation which has attracted considerable attention over the last decades. When the coefficients α and β are both positive, its linear terms describe a balance between long wave instability and short-wave stability and nonlinear terms provide a mechanism for energy transfer between wave modes. The LDG method developed in [99] can be proved to satisfy a cell entropy inequality and is therefore L^2 stable, for the general nonlinear equation (3.20). The LDG scheme is used in [99] to simulate chaotic solutions of (3.21). Figs. 3 and 4 are some of the simulation results of chaotic solutions in [99].

3.3.3 The Cahn-Hilliard equation

LDG methods have been designed in [93] for solving the Cahn-Hilliard equation in a bounded domain $\Omega\in\mathbb{R}^d$ $(d\leq 3)$

$$u_t=\nabla\cdot\Big(b(u)\nabla\big(-\gamma\Delta u+\Psi'(u)\big)\Big), \tag{3.22}$$

and for solving the Cahn-Hilliard system

$$\begin{cases} \boldsymbol{u}_t=\nabla\cdot(\boldsymbol{B}(\boldsymbol{u})\nabla\boldsymbol{\omega}), \\ \boldsymbol{\omega}=-\gamma\Delta\boldsymbol{u}+D\Psi(\boldsymbol{u}), \end{cases} \tag{3.23}$$

where $\{D\Psi(\boldsymbol{u})\}_l=\frac{\partial\Psi(\boldsymbol{u})}{\partial u_l}$ and γ is a positive constant. Here $b(u)$ is the non-negative diffusion mobility and $\Psi(u)$ is the homogeneous free energy density for the scalar case (3.22).

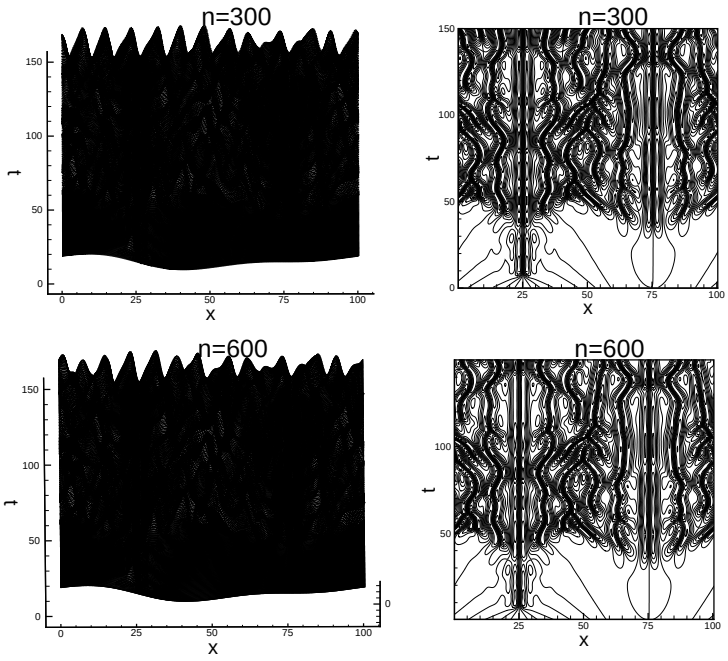

Figure 3: Reproduced from [99]. The chaotic solution of the Kuramoto-Sivashinsky equation. Periodic boundary condition in $[0,32\pi]$, P^2 elements with two different meshes using $N=300$ and $N=600$ uniform cells.

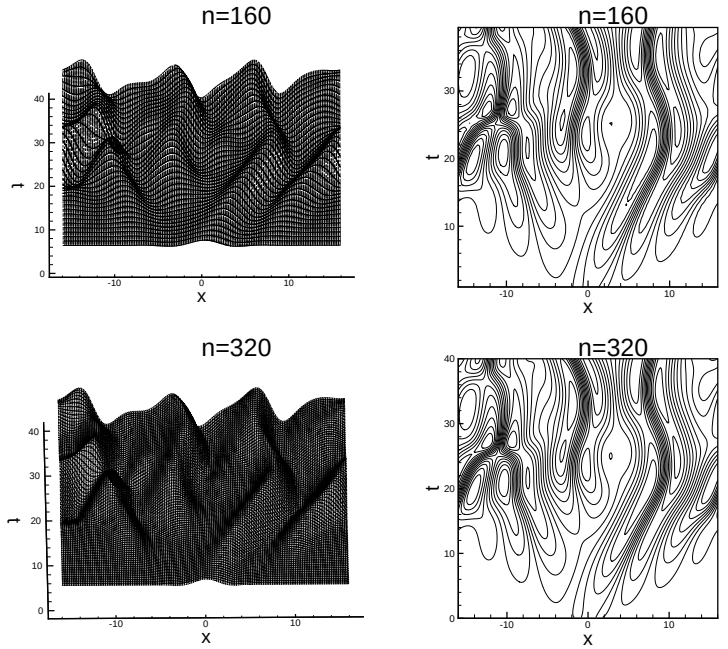

Figure 4: Reproduced from [99]. The chaotic solution of the Kuramoto-Sivashinsky equation with the Gaussian initial condition. Periodic boundary condition in [-16,16], P^2 elements with two different meshes using $N=300$ and $N=600$ uniform cells.

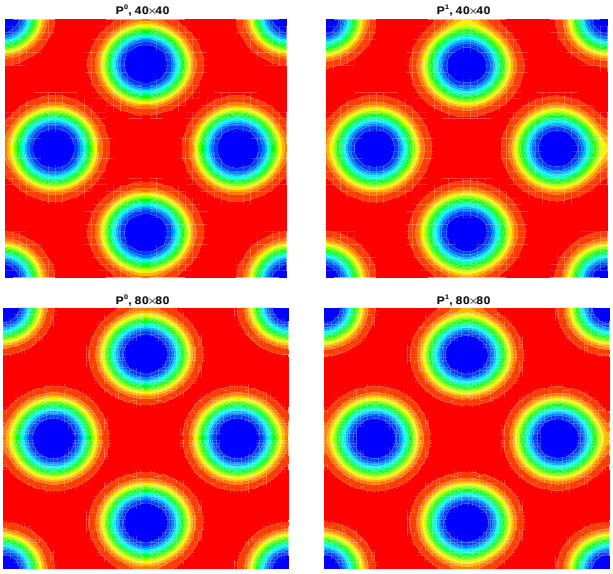

Figure 5: Reproduced from [93]. The contours of $u(x,t)$ for the Cahn-Hilliard equation (3.22) when $t=8\times10^{-5}$. P^0 and P^1 elements on the uniform mesh with 40×40 and 80×80 cells.

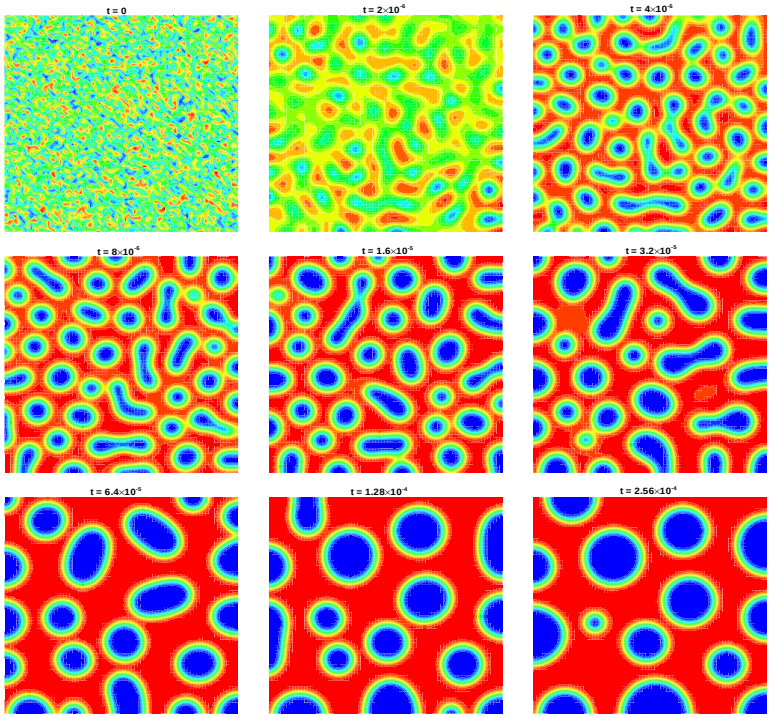

Figure 6: Reproduced from [93]. The contours evolution of $u(x,t)$ for the Cahn-Hilliard equation (3.22) at different time from a randomly perturbed initial condition with P^1 elements on the uniform mesh with 80×80 cells.

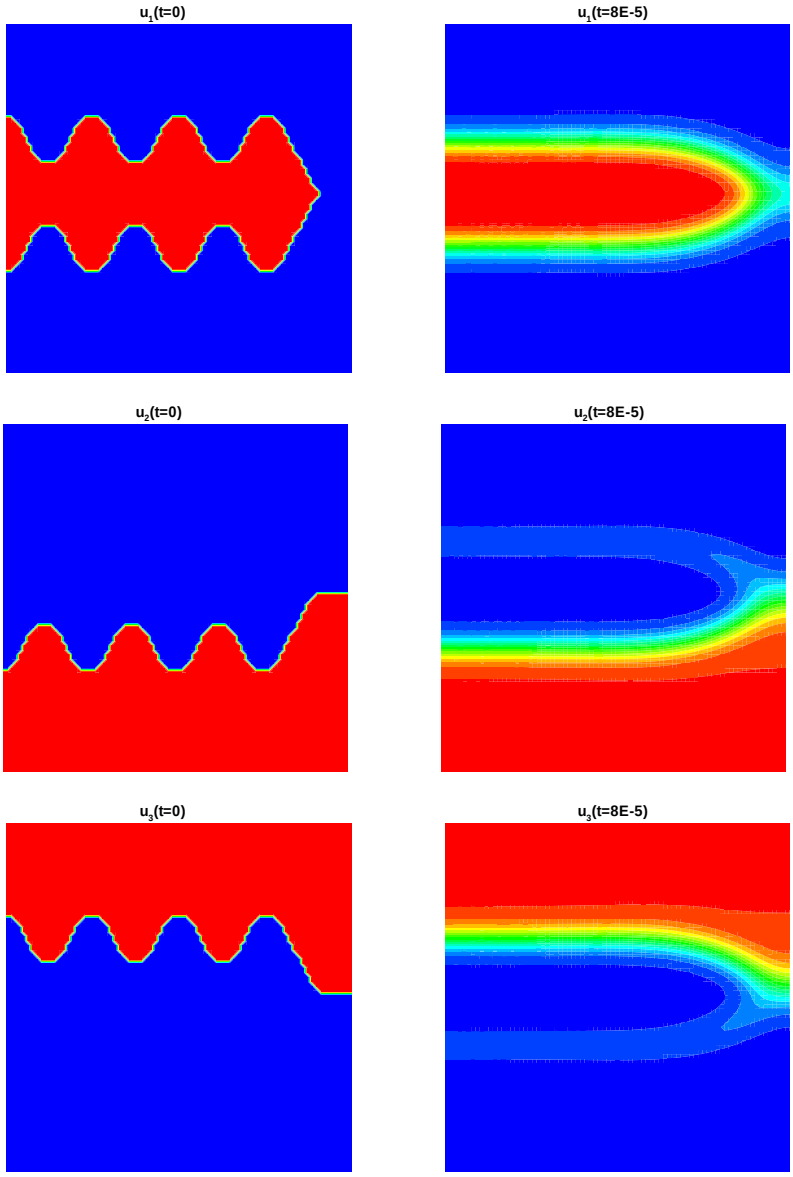

Figure 7: Reproduced from [93]. The contours of $u_1(\boldsymbol{x},t)$, $u_2(\boldsymbol{x},t)$ and $u_3(\boldsymbol{x},t)$ for the Cahn-Hilliard system (3.23) when $t=8\times10^{-5}$. P^1 elements on the uniform mesh with 80×80 cells.

For the system case (3.23), $\boldsymbol{B}(\boldsymbol{u})$ is the symmetric positive semi-definite mobility matrix and $\Psi(\boldsymbol{u})$ is the homogeneous free energy density. The proof of the energy stability for the LDG scheme is given for the general nonlinear solutions. Many simulation results are given in [93]. The numerical results for two dimensional Cahn-Hilliard equation and Cahn-Hilliard system are shown in Figs. 5, 6 and 7.

In [94], a class of LDG methods are designed for the more general Allen-Cahn/Cahn-Hilliard (AC/CH) system in $\Omega\in\mathbb{R}^d$ ($d\leq 3$)

$$\begin{cases} u_t=\nabla\cdot[b(u,v)\nabla(\Psi_u(u,v)-\gamma\Delta u)], \\ \rho v_t=-b(u,v)[\Psi_v(u,v)-\gamma\Delta v], \end{cases} \tag{3.24}$$

where γ, ρ are given constants. The mobility, $b(u,v)$, is assumed to be nonnegative and to vanish at the "pure phases". The homogeneous free energy, Ψ, is assumed to contain two terms, one for entropy contribution and the other for energy mixing. Energy stability of the LDG schemes is again proved. Simulation results are provided in [94].

3.3.4 The surface diffusion of graphs and Willmore flow of graphs equations

In [103], we designed the LDG method for the surface diffusion of graphs

$$u_t+\nabla\cdot\left(Q\left(\boldsymbol{I}-\frac{\nabla u\otimes\nabla u}{Q^2}\right)\nabla H\right)=0, \tag{3.25}$$

and the equation of Willmore flow of graphs

$$u_t+Q\nabla\cdot\left(\frac{1}{Q}\left(\boldsymbol{I}-\frac{\nabla u\otimes\nabla u}{Q^2}\right)\nabla(QH)\right)-\frac{1}{2}Q\nabla\cdot\left(\frac{H^2}{Q}\nabla u\right)=0, \tag{3.26}$$

where Q is the area element

$$Q=\sqrt{1+|\nabla u|^2}, \tag{3.27}$$

and H is the mean curvature of the domain boundary Γ

$$H=\nabla\cdot\left(\frac{\nabla u}{Q}\right). \tag{3.28}$$

There are general application areas of these models, such as body shape dynamics, surface destruction, computer data processing, image processing and so on. These two equations are both highly nonlinear fourth-order PDEs. L^2 stability and energy stability are proven for general solutions.

3.4 Porous medium equation

An LDG method for solving the porous medium equation

$$u_t=(u^m)_{xx},\quad m\geq 1 \tag{3.29}$$

is designed in [109]. This equation often occurs in nonlinear problems of heat and mass transfer, combustion theory, and flow in porous media, where u is either a concentration

or a temperature required to be nonnegative. This equation is a degenerate parabolic equation since it degenerates at the points where $u=0$. A nonnegativity preserving limiter to satisfy the physical nature of the porous medium equation is presented in [109]. The nonnegativity of the LDG method for P^0 element is proved if the initial solution is nonnegative within certain restriction on the parameters of the numerical flux. Extensive numerical results are given to show the capability of the LDG method in [109].

4 The LDG method for dispersive equations

In this section, we discuss the development of the LDG methods for the dispersive equations, such as KdV-type equations, Kadomtsev-Petviashvili equation and Zakharov-Kuznetsov equation, etc.

4.1 The LDG method for the KdV-type equations

We present the LDG method for the KdV-type equations in [104]:

$$u_t+f(u)_x+(r'(u)g(r(u)_x)_x)_x=0 \tag{4.1}$$

with an initial condition

$$u(x,0)=u_0(x) \tag{4.2}$$

and periodic boundary conditions. Here $f(u)$, $g(q)$ are arbitrary (smooth) nonlinear functions. Notice that the assumption of periodic boundary conditions is for simplicity only and is not essential: the method can be easily designed for non-periodic boundary conditions (see, e.g., [71]).

To define the LDG method, we rewrite Eq. (4.1) as a first order system:

$$u_t+f(u)_x+(r'(u)p)_x=0,\quad p-g(q)_x=0,\quad q-r(u)_x=0. \tag{4.3}$$

Now we can use the LDG method to approximate Eq. (4.3). Find u, p, $q\in V_{\Delta x}$, such that, $\forall\rho$, ϕ, $\varphi\in V_{\Delta x}$,

$$\begin{aligned}
&\int_{I_j}u_t\rho dx-\int_{I_j}(f(u)+r'(u)p)\rho_x dx+(\hat{f}+\hat{r'}\hat{p})_{j+\frac{1}{2}}\rho^-_{j+\frac{1}{2}}-(\hat{f}+\hat{r'}\hat{p})_{j-\frac{1}{2}}\rho^+_{j-\frac{1}{2}}=0,\\
&\int_{I_j}p\phi dx+\int_{I_j}g(q)\phi_x dx-\hat{g}_{j+\frac{1}{2}}\phi^-_{j+\frac{1}{2}}+\hat{g}_{j-\frac{1}{2}}\phi^+_{j-\frac{1}{2}}=0,\\
&\int_{I_j}q\varphi dx+\int_{I_j}r(u)\varphi_x dx-\hat{r}_{j+\frac{1}{2}}\varphi^-_{j+\frac{1}{2}}+\hat{r}_{j-\frac{1}{2}}\varphi^+_{j-\frac{1}{2}}=0.
\end{aligned} \tag{4.4}$$

The numerical fluxes at the boundary terms are taken as

$$\hat{f}=\hat{f}(u^-,u^+),\quad \hat{g}=\hat{g}(q^-,q^+),\quad \hat{p}=p^+,\quad \hat{r'}=\frac{r(u^+)-r(u^-)}{u^+-u^-},\quad \hat{r}=r(u^-), \tag{4.5}$$

where we have omitted the half-integer indices $j+\frac{1}{2}$ as all quantities in (4.5) are computed at the same points (i.e. the interfaces between the cells). Here $\hat{f}(u^-,u^+)$ and $-\hat{g}(q^-,q^+)$ are monotone fluxes. We remark that the choice for the fluxes (4.5) is not unique. In fact the crucial part is taking $\hat{p}$ and $\hat{r}$ from opposite sides.

Notice that, from the third equation in the scheme (4.4), we can solve q explicitly and locally (in cell I_j) in terms of u, by inverting the small mass matrix inside the cell I_j. Then, from the second equation in the scheme (4.4), we can solve p explicitly and locally (in cell I_j) in terms of q. Thus only u is the global unknown and the auxiliary variables q and p can be solved in terms of u locally.

Remark 4.1. Choice for the numerical fluxes
The upwinding principle for the numerical flux $\hat{f}(u^-,u^+)$ and $-\hat{g}(q^-,q^+)$ is essential to ensure stability for the odd derivative which correspond to waves. For other numerical fluxes, symmetric treatment is the guiding principle to ensure stability.

Remark 4.2. L^2 stability
For the scheme (4.4) with the numerical fluxes (4.5), cell entropy inequality and L^2 stability can be proved.

Remark 4.3. Error estimates
The sub-optimal $\mathcal{O}(h^{k+\frac{1}{2}})$ error estimates in L^2 norm can be obtained for the smooth solution of the equation [100, 104]

$$u_t+f(u)_x+u_{xxx}=0. \tag{4.6}$$

Remark 4.4. Multi-dimensional case
For the general multi-dimensional nonlinear case

$$u_t+\sum_{i=1}^{d}f_i(u)_{x_i}-\sum_{i=1}^{d}\left(r_i'(u)\sum_{j=1}^{d}g_{ij}(r_i(u)x_i)_{x_j}\right)_{x_i}=0,\quad d\geq 1, \tag{4.7}$$

the LDG scheme can also be designed in the similar way and the cell entropy and L^2 stability can be proved in any spatial dimension and any triangulation, for any order of accuracy in [104]. Error estimates of $\mathcal{O}(h^k)$ in L^2 norm for P^k elements in 2D are obtained in [100].

In Table 3, we show the classical soliton solution of the nonlinear KdV equation [104]

$$u_t-3u_x^2+u_{xxx}=0, \tag{4.8}$$

with an initial condition $u(x,0)=-2\text{sech}^2(x)$ for $-10\leq x\leq 12$. The exact solution is given by $u(x,t)=-2\text{sech}^2(x-4t)$. We clearly observe an accuracy of $\mathcal{O}(h^{k+1})$ when piecewise P^k elements are used.

In [104], this LDG method is used to study the dispersion limit of the Burgers equation

$$u_t+u_x^2+\varepsilon u_{xxx}=0, \tag{4.9}$$

for which the third derivative dispersion term in (4.1) has a small coefficient which tends to zero. Fig. 8 show the zero dispersion limit results in [104].

Table 3: Reproduced from [104]. Accuracy results for the KdV equation (4.8). Periodic boundary conditions. L^∞ errors. Uniform meshes with N cells. LDG methods with $k=0,1,2,3$. $t=0.5$.

k		N=40	N=80		N=160		N=320	
		error	error	order	error	order	error	order
0	L^2	2.5292E-01	1.9098E-01	0.40	1.3019E-01	0.55	7.9780E-02	0.71
	L^∞	9.0170E-01	6.8651E-01	0.39	4.6405E-01	0.56	2.8531E-01	0.70
1	L^2	2.6512E-02	4.6652E-03	2.50	1.0108E-03	2.20	2.5906E-04	1.96
	L^∞	1.4748E-01	3.4625E-02	2.09	1.1840E-02	1.55	3.3239E-03	1.83
2	L^2	1.5317E-03	1.8083E-04	3.08	2.2642E-05	2.99	2.8335E-06	2.99
	L^∞	1.7486E-02	2.7505E-03	2.66	3.5575E-04	2.95	4.4397E-05	3.00
3	L^2	2.0631E-04	1.3981E-05	3.88	8.9054E-07	3.97	5.6029E-08	3.99
	L^∞	2.0155E-03	2.1462E-04	3.23	1.4461E-05	3.89	9.1140E-07	3.98

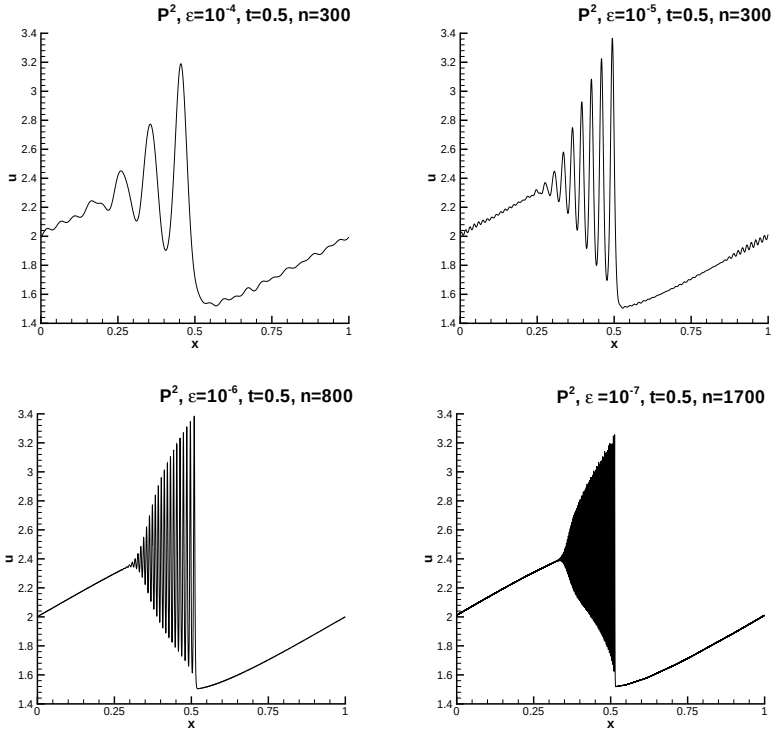

Figure 8: Reproduced from [104]. Zero dispersion limit of conservation laws. Solutions of Eq. (4.9) and periodic boundary conditions in [0,1] using P^2 elements at $t=0.5$. Top left: $\epsilon=10^{-4}$ with 300 cells; top right: $\epsilon=10^{-5}$ with 300 cells; bottom left: $\epsilon=10^{-6}$ with 800 cells; bottom right: $\epsilon=10^{-7}$ with 1700 cells.

4.2 The LDG scheme of the Kadomtsev-Petviashvili (KP) and Zakharov-Kuznetsov (ZK) equation

The KP equation

$$(u_t+6uu_x+u_{xxx})_x+3\sigma^2u_{yy}=0, \tag{4.10}$$

where $\sigma^2=\pm1$, are generalizations of the one-dimensional KdV equations and are important models for water waves. Because of the x-derivative for the u_t term, Eq. (4.10) is well-posed only in a function space with a global constraint, hence it is difficult to design an efficient LDG scheme which relies on local operations. This equation is equivalent to

$$u_t+6uu_x+u_{xxx}+3\sigma^2\partial_x^{-1}u_{yy}=0, \tag{4.11}$$

where the non-local operator $\partial_x^{-1}u_{yy}$ makes the equation well-posed only in the restricted space

$$\mathcal{V}(R^2)=\left\{f:\int_{R^2}(1+\xi^2+\frac{\eta^2}{\xi^2})|\hat{f}(\xi,\eta)|^2d\xi d\eta<\infty\right\}.$$

We have designed an LDG scheme for (4.10) in [98] by carefully choosing locally supported bases which satisfy the global constraint needed by the solution of (4.11). We give the piecewise polynomial basis functions of the space, which satisfy the constraint from the PDE with a non-local operator and at the same time have the local property of the discontinuous Galerkin methods. Details related to the implementation are also described in [98]. The LDG scheme is L^2 stable for the fully nonlinear equation (4.10). Numerical simulations in Figs. 9 and 10 are performed in [98] for both the KP-I equations ($\sigma^2=-1$ in (4.10)) and the KP-II equations ($\sigma^2=1$ in (4.10)).

The Zakharov-Kuznetsov equation

$$u_t+(3u^2)_x+u_{xxx}+u_{xyy}=0 \tag{4.12}$$

is another generalization of the one-dimensional KdV equations. An LDG scheme is designed for (4.12) in [98] which is proved to satisfy a cell entropy inequality and to be L^2 stable. An L^2 error estimate is given in [100]. Various nonlinear waves have been simulated by this scheme in [98]. The direct collision of two dissimilar pulses solution is shown in Fig. 11.

4.3 Applications of the LDG method for other dispersive equations

4.3.1 Fifth order convection dispersion equations

An LDG scheme for solving the following fifth order convection dispersion equation

$$u_t+\sum_{i=1}^{d}f_i(u)_{x_i}-\sum_{i=1}^{d}(g_i(u_{x_ix_i})_{x_ix_ix_i}=0,\quad d\geq1, \tag{4.13}$$

where $f_i(u)$ and $g_i(q)$ are arbitrary functions, was designed in [105]. The numerical fluxes are chosen following the same upwinding and alternating flux principle similar to the third order KdV type equations (4.1), see (4.5). A cell entropy inequality and the L^2 stability of the LDG scheme for the nonlinear equation (4.13) can be proved [105], which again do not depend on the smoothness of the solution of (4.13), the order of accuracy of the scheme, or the triangulation. Stable LDG schemes for similar equations with seventh or higher derivatives can also be designed along similar lines.

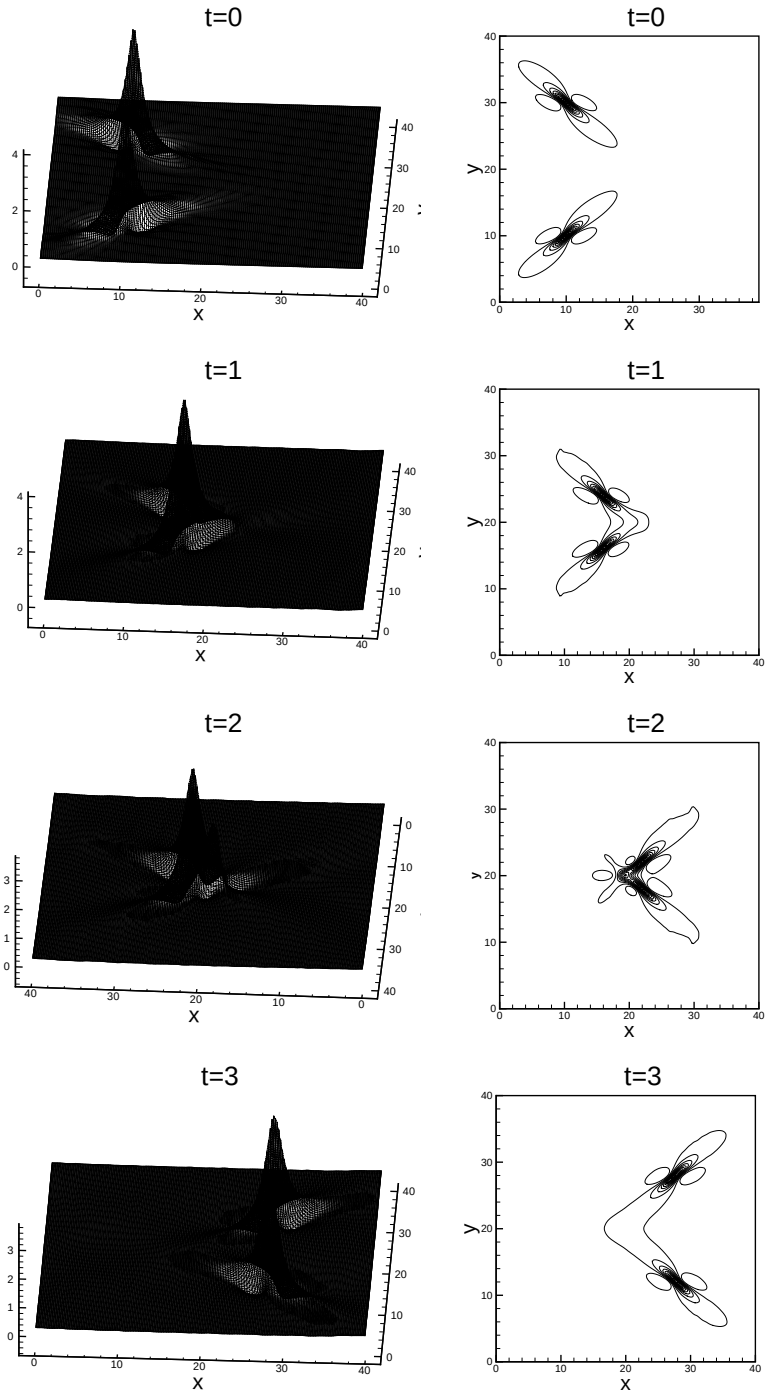

Figure 9: Reproduced from [98]. Indirect collision of two lump-type pulse of KP-I equation, $\mu_1^2=\mu_2^2=1$, $\lambda_1=-1$, $\lambda_2=1$, $x_1=10$, $y_1=10$, $x_2=10$, $y_2=30$. Periodic boundary condition in both x and y directions in $[0,40]\times[0,40]$. P^2 elements with 160×160 uniform cells.

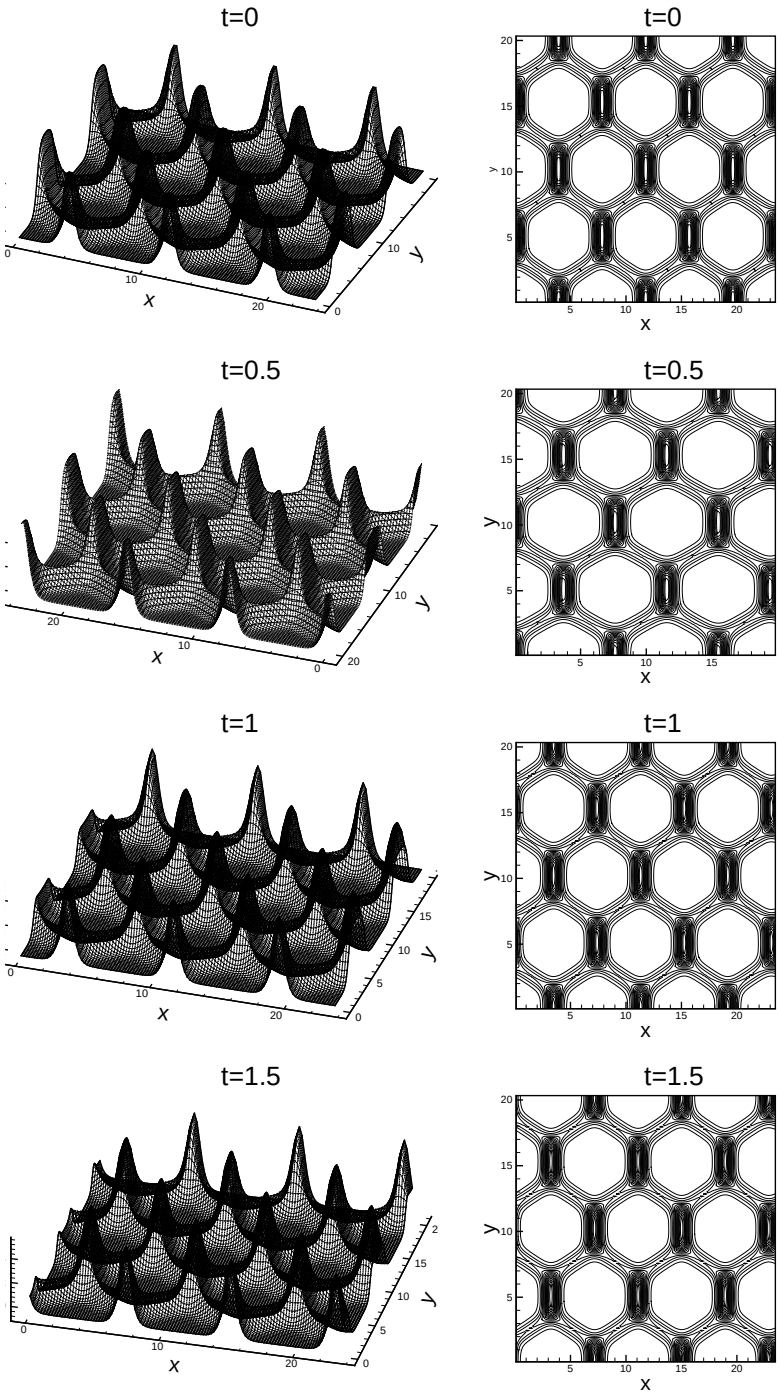

Figure 10: Reproduced from [98]. A two-phase solution for KP-II equation, with parameters: $b=-2$, $\lambda=0.4$, $b\lambda^2+d=-2$, $\mu_1=\mu_2=0.8$, $\nu_1=-\nu_2=0.6155175$, $\omega_1=\omega_2=-5.924798$, $\phi_{1,0}=0$ and $\phi_{2,0}=0$. Periodic boundary condition in both x and y directions in $[0,6\pi/\mu_1]\times[0,2\pi/\nu_1]$. P^2 elements with 120×120 uniform cells.

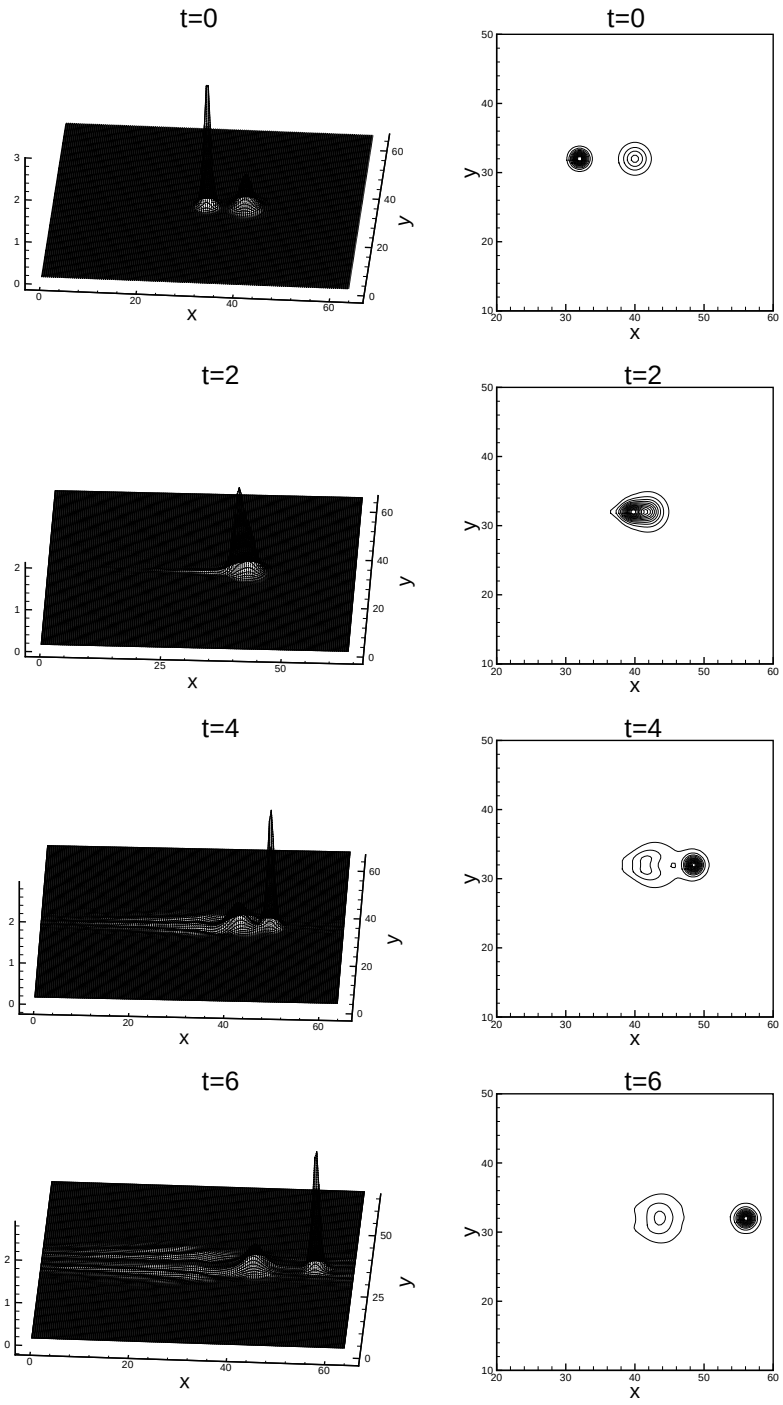

Figure 11: Reproduced from [98]. Direct collision of two dissimilar pulses solution for the ZK equation (4.12). $c_1=4,\ c_2=1,\ x_1=32,\ y_0=32,\ x_2=40,\ y_2=32$. Periodic boundary conditions in both x and y directions in $[0,64]\times[0,64]$. P^2 elements with 160×160 uniform cells

4.3.2 The fifth-order KdV type equations

LDG methods for solving the fifth-order KdV type equations

$$u_t+f(u)_x+(r'(u)g(r(u)_x)_x)_x+(s'(u)h(s(u)_{xx})_{xx})_x=0, \tag{4.14}$$

where $f(u)$, $r(u)$, $g(q)$, $s(u)$ and $h(p)$ are arbitrary functions, have been designed in [96]. The design of numerical fluxes follows the same lines as that for the KdV type equation (4.1). A cell entropy inequality and the L^2 stability of the LDG scheme for the nonlinear equation (4.14) can be proved [96], which again do not depend on the smoothness of the solution of (4.14) and the order of accuracy of the scheme. The LDG scheme is used in [96] to simulate the solutions of the Kawahara equation, the generalized Kawahara equation, Ito's fifth-order mKdV equation, and a fifth-order KdV type equations with high nonlinearities, which are all special cases of the equations represented by (4.14).

A special case is the Kawahara equation

$$u_t+uu_x+u_{xxx}-\delta u_{xxxxx}=0. \tag{4.15}$$

In Fig. 12, we show the result with the compact initial condition

$$u_0(x)=\begin{cases} A\cos^2(Bx-C) & |Bx-C|\le \pi/2, \\ 0 & \text{otherwise.} \end{cases} \tag{4.16}$$

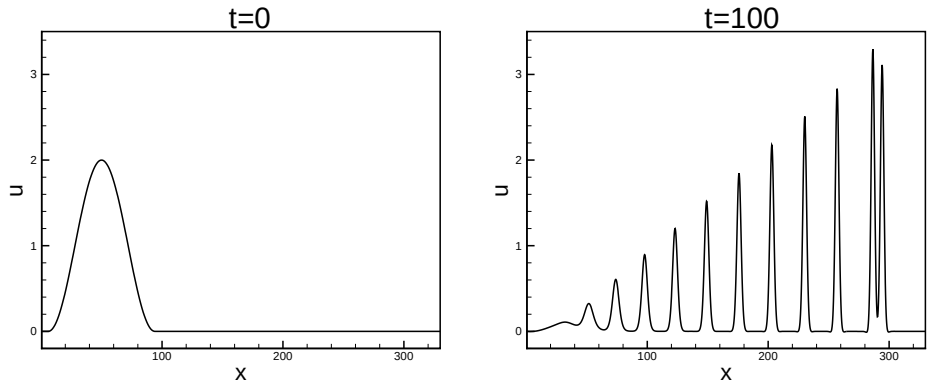

Figure 12: Reproduced from [96]. The pulsating multiplet solution of Eq. (4.15) for $\delta=0.5$ in [0,330] using P^2 elements with 1500 cells, where $A=2$, $B=1/28$ and $C=50/28$.

4.3.3 The fully nonlinear $K(m,n)$ and $K(n,n,n)$ equations

LDG methods for solving the $K(m,n)$ equations

$$u_t+(u^m)_x+(u^n)_{xxx}=0, \tag{4.17}$$

where m and n are positive integers, have been designed in [67]. These $K(m,n)$ equations were introduced by Rosenau and Hyman in [80] to study the so-called compactons,

namely the compactly supported solitary waves solutions. For the special case of $m=n$ with an odd positive integer, it is possible to design LDG schemes which are stable in the L^{m+1} norm. For other cases, LDG schemes can be designed based on a linearized stability analysis, which perform well in numerical simulation for the fully nonlinear equation (4.17).

LDG methods for solving the fifth-order fully nonlinear $K(n,n,n)$ equations

$$u_t+(u^n)_x+(u^n)_{xxx}+(u^n)_{xxxxx}=0, \tag{4.18}$$

where n is a positive integer, have been designed in [96]. The design of numerical fluxes follows the same lines as that for the $K(m,n)$ equations (4.17). For odd n, stability in the L^{n+1} norm of the resulting LDG scheme can be proved for the nonlinear equation (4.18) [96]. This scheme is used to simulate compacton propagation in [96].

4.3.4 The KdV-Burgers type (KdVB) equations

LDG methods for solving the KdV-Burgers type (KdVB) equations

$$u_t+f(u)_x-(a(u)u_x)_x+(r'(u)g(r(u)_x)_x)_x=0, \tag{4.19}$$

where $f(u)$, $a(u)$, $r(u)$ and $g(p)$ are arbitrary functions, have been designed in [96]. The design of numerical fluxes follows the same lines as that for the convection diffusion equation (3.8) and for the KdV type equation (4.1). A cell entropy inequality and the L^2 stability of the LDG scheme for the nonlinear equation (4.19) can be proved [96], which again do not depend on the smoothness of the solution of (4.19) and the order of accuracy of the scheme. The LDG scheme is used in [96] to study different regimes when one of the dissipation and the dispersion mechanisms dominates, and when they have comparable influence on the solution. An advantage of the LDG scheme designed in [96] is that it is stable regardless of different class of dominant operators (convection, diffusion, or dispersion).

A special case is the KdV-Burgers equation

$$u_t+\varepsilon uu_x-\alpha u_{xx}+\beta u_{xxx}=0. \tag{4.20}$$

We fix $\varepsilon=0.2$ and $\beta=0.1$, then change α. The results are shown in Fig. 13.

4.3.5 The Ito-type coupled KdV equations

In [99] we have developed an LDG method to solve the Ito-type coupled KdV equations

$$\begin{aligned} &u_t+\alpha uu_x+\beta vv_x+\gamma u_{xxx}=0,\\ &v_t+\beta(uv)_x=0, \end{aligned} \tag{4.21}$$

where α, β and γ are arbitrary constants. An L^2 stability is proved for the LDG method. Simulation for the solution of (4.21) in which u behaves like a dispersive wave solution and v behaves like a shock wave solution is performed in [99] using the LDG scheme. Fig. 14 plots the solution u which behaves like a dispersive wave solution, while Fig. 15 plots the solution v which behaves like a shock wave solution.

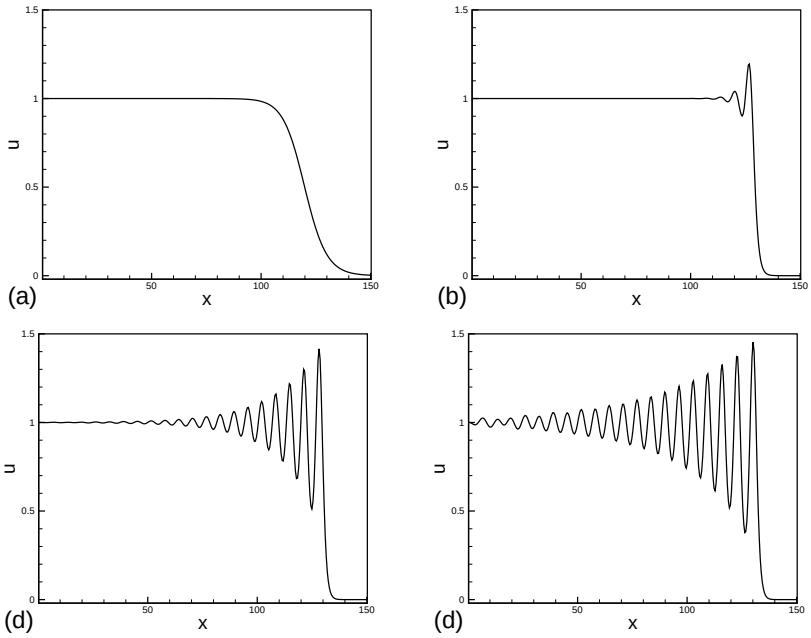

Figure 13: Reproduced from [96]. KdVB type solutions at time $t=800$, $0\leq x\leq 150$, $d=5$, $x_0=50$, $\varepsilon=0.2$ and $\beta=0.1$. (a) $\alpha=0.5$, P^1 elements with 320 cells; (b) $\alpha=0.05$, P^1 elements with 320 cells; (c) $\alpha=0.01$, P^1 elements with 320 cells; (d) $\alpha=0.005$, P^1 elements with 320 cells.

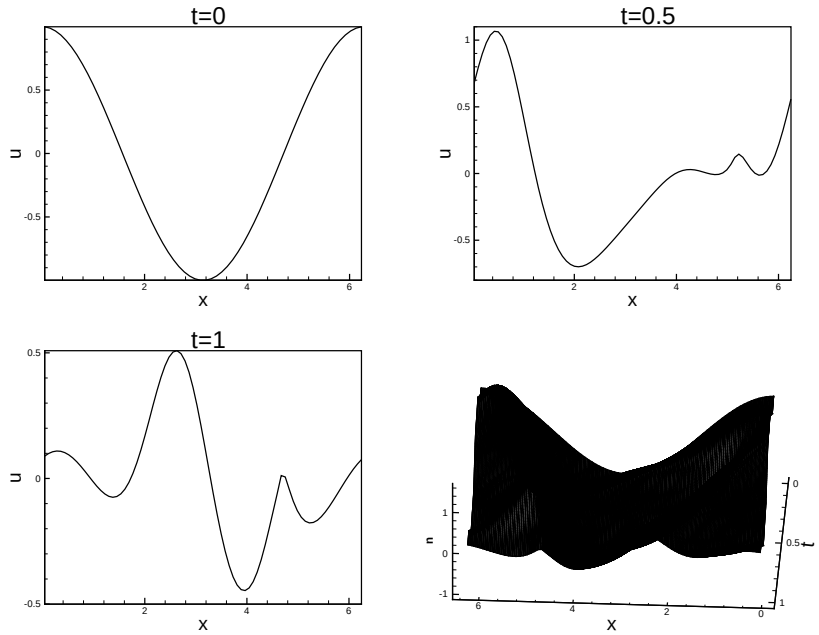

Figure 14: Reproduced from [99]. Numerical results of u for the Ito's equation (4.21). Periodic boundary condition in $[0,2\pi]$, P^2 elements with 80 cells.

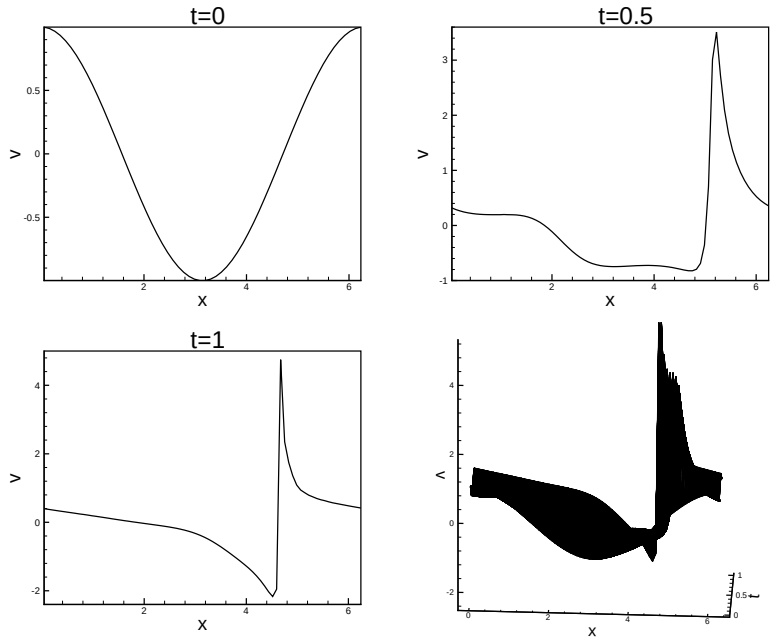

Figure 15: Reproduced from [99]. Numerical results of v for the Ito's equation (4.21). Periodic boundary condition in $[0,2\pi]$, P^2 elements with 80 cells.

5 Additional topics of the LDG method

In this section, we discuss some additional topics related to the development of the LDG methods, including nonlinear Schrödinger equation, integrable model equation for shallow water waves and multi-scale problems.

5.1 The nonlinear Schrödinger (NLS) equation

In [97], LDG methods are designed for the generalized nonlinear Schrödinger (NLS) equation

$$iu_t+u_{xx}+i(g(|u|^2)u)_x+f(|u|^2)u=0, \tag{5.1}$$

the two-dimensional version

$$iu_t+\Delta u+f(|u|^2)u=0, \tag{5.2}$$

and the coupled nonlinear Schrödinger equation

$$\begin{cases} iu_t+i\alpha u_x+u_{xx}+\beta u+\kappa v+f(|u|^2,|v|^2)u=0, \\ iv_t-i\alpha v_x+v_{xx}-\beta u+\kappa v+g(|u|^2,|v|^2)v=0, \end{cases} \tag{5.3}$$

where $f(u)$ and $g(u)$ are arbitrary (smooth) nonlinear real functions and α, β, κ are real constants. With suitable choices of the numerical fluxes, the resulting LDG schemes

are proved to satisfy a cell entropy inequality and L^2 stability and L^2 error estimate of $\mathcal{O}(h^{k+\frac{1}{2}})$ for the linearized version [97]. The LDG scheme is used in [97] to simulate the soliton propagation and interaction, and the appearance of singularities. The easiness of h-p adaptivity of the LDG scheme and rigorous stability for the fully nonlinear case make it an ideal choice for the simulation of Schrödinger equations, for which the solutions often have localized structures such as a point singularity. In [73], Lu et al. also presented LDG methods for the time dependent Schrödinger equation. A numerical flux is constructed to preserve the conservative property for the density of the particle described.

We show the double soliton collision of the NLS equation

$$iu_t+u_{xx}+2|u|^2u=0 \tag{5.4}$$

in Fig. 16.

Singular solutions for the two-dimensional NLS equation

$$iu_t+u_{xx}+u_{yy}+|u|^2u=0, \tag{5.5}$$

with the initial condition

$$u(x,y)=(1+\sin x)(2+\sin y), \tag{5.6}$$

and a periodic boundary condition are shown in Fig. 17. Strong evidence of a singularity in finite time is obtained, although there is no rigorous proof of breakdown in this case.

5.2 The Camassa-Holm (CH) equation

An LDG method for solving the Camassa-Holm (CH) equation

$$u_t-u_{xxt}+2\kappa u_x+3uu_x=2u_xu_{xx}+uu_{xxx}, \tag{5.7}$$

where κ is a constant, is designed in [101]. Because of the u_{xxt} term, the design of an LDG method is non-standard. The non-local term u_{xxt} increases the difficulty in designing an efficient and stable LDG method significantly. By a careful choice of the numerical fluxes, we obtain an LDG scheme which can be proved to satisfy a cell entropy inequality and to be L^2 stable [101]. We have also obtained a sub-optimal $\mathcal{O}(h^k)$ error estimate in L^2 norm in [101]. In Figs. 18 and 19, we show the peak profile propagation and the break up of plateau traveling wave of the CH equation.

5.3 The Hunter-Saxton (HS) equation

In [102], LDG methods are designed for the Hunter-Saxton (HS) equation

$$u_{xxt}+2u_xu_{xx}+uu_{xxx}=0, \tag{5.8}$$

its regularization with viscosity

$$u_{xxt}+2u_xu_{xx}+uu_{xxx}-\varepsilon_1u_{xxxx}=0, \tag{5.9}$$

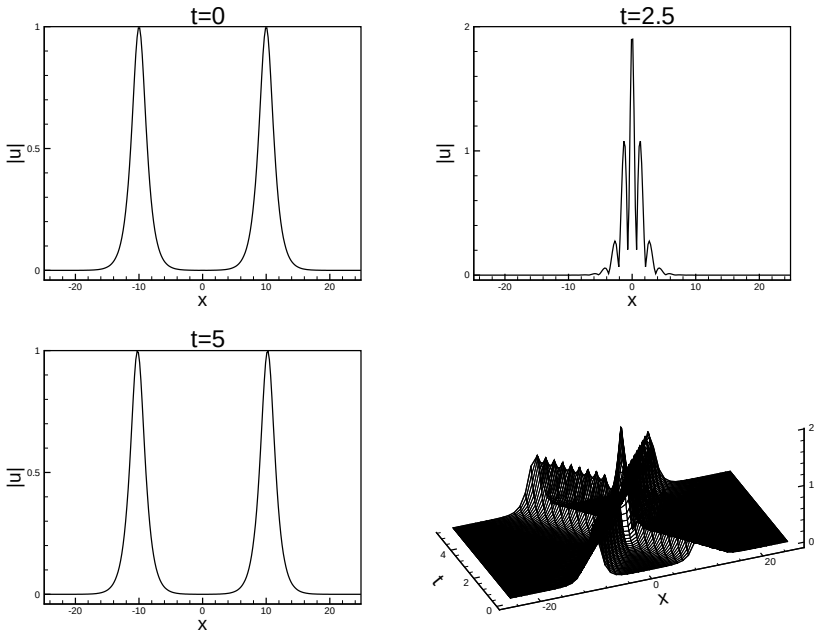

Figure 16: Reproduced from [97]. The double soliton collision of Eq. (5.4). $c_1=4$, $x_1=-10$, $c_2=-4$, $x_2=10$. Periodic boundary condition in $[-25,25]$. P^2 elements with 250 uniform cells.

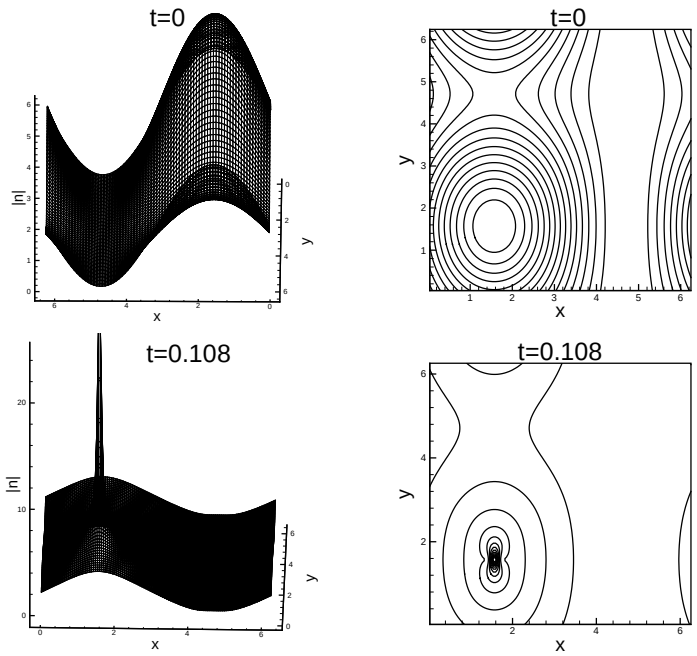

Figure 17: Reproduced from [97]. The singular solution of Eq. (5.5) with initial condition (5.6). Periodic boundary condition in $[0,2\pi]$. P^2 elements with 120×120 uniform cells.

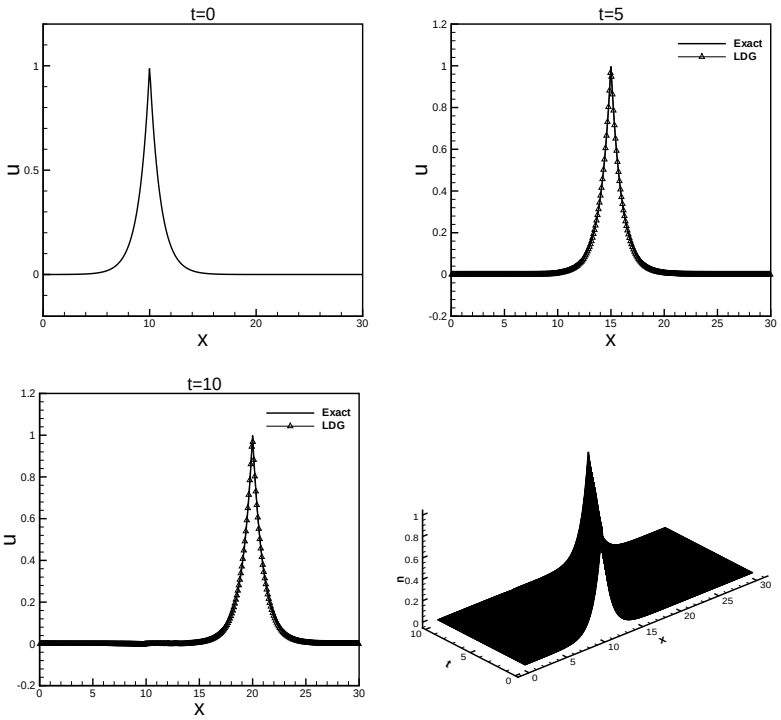

Figure 18: Reproduced from [101]. The peak profile of the CH equation (5.7). Periodic boundary condition in $[0,30]$. P^5 elements and a uniform mesh with $N=320$ cells.

and its regularization with dispersion

$$u_{xxt}+2u_xu_{xx}+uu_{xxx}-\varepsilon_2u_{xxxxx}=0, \tag{5.10}$$

where $\varepsilon_1\geq 0$ and ε_2 are small constants. This equation arises in two different physical contexts in two nonequivalent variational forms. It is the high frequency limit of the Camassa-Holm equation, which is an integrable model equation for shallow water waves. The nonlinear terms in the HS equation are similar to those in the Camassa-Holm equation. Even though the method developed in [101] gives us a hint on how to treat these nonlinear derivative terms, the different solution property of the HS equation gives birth to new difficulties. When u_x becomes discontinuous, a special numerical treatment for the derivative is needed. LDG methods for the HS type equations are designed and a rigorous proof for the energy stability are given in [102].

5.4 Multi-scale problems

In [106], DG methods based on non-polynomial approximation spaces are developed for numerical solution of time dependent hyperbolic, parabolic, steady-state hyperbolic and elliptic PDEs. The algorithm is based on approximation spaces consisting of non-polynomial elementary functions such as exponential functions, trigonometric functions,

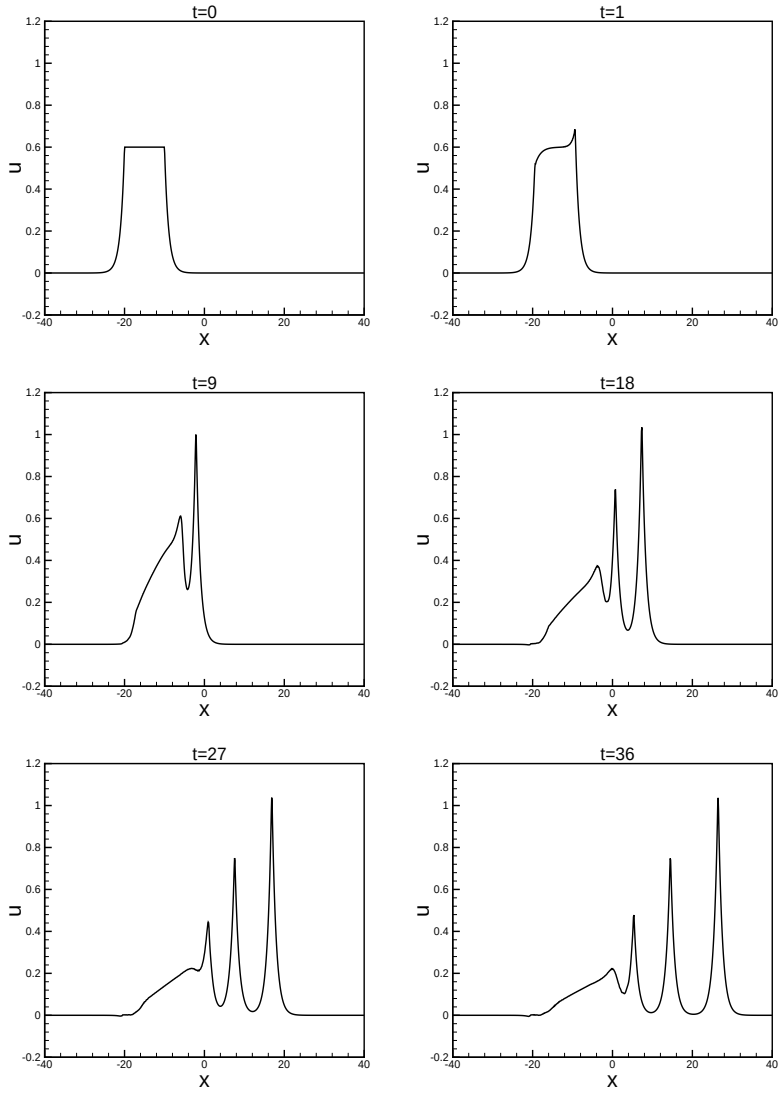

Figure 19: Reproduced from [101]. The break up of plateau traveling wave of the CH equation (5.7). Periodic boundary condition in $[-40,40]$. P^2 elements and a uniform mesh with $N=800$ cells.

etc., with the objective of obtaining better approximations for specific types of PDEs and initial and boundary conditions. L^2 stability and error estimates can be obtained when the approximation space is suitably selected. Numerical examples with a careful selection of the approximation space to fit individual PDE and initial and boundary conditions show more accurate results than the DG methods based on the polynomial approximation spaces of the same order of accuracy.

This technique is used to solve the elliptic multi-scale problem based on the DG

method in [107]. They consider the following elliptic multi-scale problem

$$-\nabla\cdot(a^{\varepsilon}(x)\nabla u)=f(x), \tag{5.11}$$

where the coefficient $a^{\varepsilon}(x)$ is an oscillatory function involving a small scale ε, for example it could be $a^{\varepsilon}(x)=a(x,x/\varepsilon)$ and the force function $f(x)$ does not involve this small scale. The main ingredient of this method is to use a non-polynomial multi-scale approximation space in the DG method to capture the multi-scale solutions using coarse meshes without resolving the fine-scale structure of the solution. Analysis on the approximation, stability and error estimates, and numerical results are presented in [107].

In [91], Wang and Shu discuss the one-dimensional stationary Schrödinger Poisson problem

$$\begin{cases} -\frac{\hbar^2}{2m}\varphi_p''-qV\varphi_p=E_p^a\varphi_p,\ (p\geq 0), \\ \hbar\varphi_p'(a)+ip\varphi_p(a)=2ip;\quad \hbar\varphi_p'(b)=ip_b\varphi_p(b), \end{cases} \tag{5.12}$$

where m is the effective mass (assumed to be constant in the device), q is the elementary positive charge of the electron, V is the total electrostatic potential in the device and

$$p_b=\sqrt{p^2+2qm(V_b-V_a)},\quad E_p^a=\frac{p^2}{2m}-qV_a.$$

An explicit formula for the phase factor of wave functions from WKB asymptotic analysis can be obtained. Based on the development for LDG methods for the non-polynomial basis functions in [106], the work in [91] combines the WKB approach with the LDG method by using exponential wave approximation spaces. It provides an important reduction of both the computational cost and memory in solving the Schrödinger equation. This fast solver is applied to the simulation of the resonant tunneling diode where the Schrödinger equation needs to be simulated repeatedly. In Table 4, the results for the linear Schrödinger equation under two energies are shown. WKB-LDG method present a round-off error in the linear case. LDG P^1 has a second order convergence and LDG P^2 has a third order convergence in L^2 norm.

Table 4: Reproduced from [91]. Results in the linear case with exact solution.

	N	L^2 error	N	L^2 error
	$E=0.0895eV$		$E=0.046072eV$	
WKB-LDG	13	4.63E-14	13	1.57E-16
	39	1.86E-12	39	2.34E-13
LDG P^1	135	2.66E-4	135	2.00E-5
	1350	1.76E-6	1350	1.84E-7
LDG P^2	135	6.00E-6	135	4.90E-7
	1350	6.13E-9	1350	4.94E-10

6 Time discretization

The application of the DG or LDG method discretizes the spatial variables and generates a large coupled system of ordinary differential equations (ODEs). One would then need to use a suitable ODE solver to discretize the time variable. For hyperbolic conservation laws and convection dominated convection diffusion equations, explicit and nonlinearly stable Runge-Kutta time discretizations [55, 85] are suitable choices. The resulting fully discretized scheme, termed Runge-Kutta DG (RKDG) method [37], are stable, efficient and accurate for solving such convection or convection dominated problems. However, for PDEs with higher order spatial derivatives, especially when the coefficients in front of these higher order spatial derivative terms are not small, such explicit and local time discretization suffers from extremely small time step restriction for stability, of the form $\Delta t \leq C\Delta x^p$ where p is the order of the PDE, due to the stiffness of the spatial LDG operator which approximates both the lower and higher order spatial derivatives. Often, such a small time step is not needed for the purpose of accuracy and is purely an artifact of the explicit time discretization technique. It would therefore be desirable to use either nonlocal or implicit time discretization techniques to alleviate this problem.

In [92], three different time discretization techniques for solving the stiff ODEs resulting from a LDG spatial discretization to PDEs with higher order spatial derivatives were explored. These are the semi-implicit spectral deferred correction (SDC) method, the additive Runge-Kutta (ARK) method and the exponential time differencing (ETD) method. Numerical experiments are performed to verify that all three methods are efficient in discretizing the LDG schemes in time, allowing time steps $\Delta t = \mathcal{O}(\Delta x)$ rather than the much more restrictive $\Delta t = \mathcal{O}(\Delta x^k)$ of explicit time discretizations for k-th order PDEs. In particular, the SDC method has the advantage of easy implementation for arbitrary order of accuracy. In the following, we give a brief introduction to these three methods.

6.1 The spectral deferred correction method

Dutt, Greengard and Rokhlin presented a new variation of the classical method of deferred correction, called the spectral deferred correction (SDC) method, in [49]. It is based on low order time integration methods, which are corrected iteratively, with the order of accuracy increased by one for each additional iteration. Attractively, we can split stiff and non-stiff terms as needed and treat them differently (implicitly for the stiff terms and explicitly for the non-stiff terms). Minion presented the semi-implicit SDC (SISDC) method in [74].

Consider the ODE system

$$\begin{cases} u_t = F(t,u(t)), \quad t \in [0,T], \\ u(0) = u_0, \end{cases} \tag{6.1}$$

where $u_0, u(t) \in \mathbb{C}^n$ and $F : \mathbb{R} \times \mathbb{C}^n \longrightarrow \mathbb{C}^n$. $F \in C^1(\mathbb{R} \times \mathbb{C}^n)$, which is sufficient to guarantee local existence and uniqueness of the solution to (6.1).

Suppose now the time interval $[0,T]$ is divided into N intervals by the partition $0=t_0<t_1<\cdots<t_n<\cdots<t_N=T$. Let $\Delta t_n\equiv t_{n+1}-t_n$ and u_n denotes the numerical approximation of $u(t_n)$, with $u_0=u(0)$.

Rewrite (6.1) into an integral form in the subinterval $[t_n,t_{n+1}]$:

$$u(t_{n+1})=u(t_n)+\int_{t_n}^{t_{n+1}}F(\tau,u(\tau))d\tau. \tag{6.2}$$

Then divide the time interval $[t_n,t_{n+1}]$ into P subintervals by choosing the points $t_{n,m}$ for $m=0,1,\cdots,P$ such that $t_n=t_{n,0}<t_{n,1}<\cdots<t_{n,m}<\cdots<t_{n,P}=t_{n+1}$. Let $\Delta t_{n,m}=t_{n,m+1}-t_{n,m}$ and $u_{n,m}^k$ denotes the k^{th} order approximation to $u(t_{n,m})$. To avoid the instability of approximation at equispaced nodes for high order accuracy, the points $\{t_{n,m}\}_{m=0}^P$ are chosen to be the Chebyshev Gauss-Lobatto nodes on $[t_n,t_{n+1}]$. We can also use the Legendre Gauss-Lobatto nodes, or Chebyshev or Legendre Gauss-Radau or Gauss nodes. Starting from u_n, we give the algorithm to calculate u_{n+1} in the following.

Compute the initial approximation

$u_{n,0}^1=u_n$.

For non-stiff/stiff problems, use the forward/backward Euler method to compute a first order accurate approximate solution u^1 at the nodes $\{t_{n,m}\}_{m=1}^P$.

For $m=0,\cdots,P-1$

1. For non-stiff problems,

$$u_{n,m+1}^1=u_{n,m}^1+\Delta t_{n,m}F(t_{n,m},u_{n,m}^1). \tag{6.3}$$

2. For stiff problems,

$$u_{n,m+1}^1=u_{n,m}^1+\Delta t_{n,m}F(t_{n,m+1},u_{n,m+1}^1). \tag{6.4}$$

Compute successive corrections

For $k=1,\cdots,K$

$u_{n,0}^{k+1}=u_n$.

For $m=0,\cdots,P-1$

1. For non-stiff problems, with $0\le\theta\le1$,

$$u_{n,m+1}^{k+1}=u_{n,m}^{k+1}+\theta\Delta t_{n,m}(F(t_{n,m},u_{n,m}^{k+1})-F(t_{n,m},u_{n,m}^k))+I_m^{m+1}(F(t,u^k)), \tag{6.5}$$

2. For stiff problems, with $\frac{1}{2}\le\theta\le1$,

$$\begin{aligned}u_{n,m+1}^{k+1}=u_{n,m}^{k+1}&+\theta\Delta t_{n,m}\Big(F(t_{n,m+1},u_{n,m+1}^{k+1})-F(t_{n,m+1},u_{n,m+1}^k)\Big)\\&+I_m^{m+1}(F(t,u^k)),\end{aligned} \tag{6.6}$$

where $I_m^{m+1}(F(t,u^k))$ is the integral of the P-th degree interpolating polynomial on the $P+1$ points $(t_{n,m},F(t_{n,m},u_{n,m}^k))_{m=0}^P$ over the subinterval $[t_{n,m},t_{n,m+1}]$, which is the numerical quadrature approximation of

$$\int_{t_{n,m}}^{t_{n,m+1}} F(\tau,u(\tau))d\tau. \tag{6.7}$$

Finally we have $u_{n+1}=u_{n,P}^{K+1}$.

6.2 Additive Runge-Kutta methods

When the right hand side $F(t,u)$ of the ODE (6.1) can be written as the sum of a non-stiff term $F_N(t,u)$ and a stiff term $F_S(t,u)$, we have

$$\begin{cases} u_t=F_N(t,u(t))+F_S(t,u(t)), \quad t\in[0,T], \\ u(0)=u_0. \end{cases} \tag{6.8}$$

Following the work [5, 65], the ARK methods are used to solve equation (6.8). They are given in the following form

$$u^{(i)}=u_n+\Delta t\sum_{j=0}^{i-1}a_{ij}^{[N]}F_N(t_n+c_j\Delta t,u^{(j)})+\Delta t\sum_{j=0}^{i}a_{ij}^{[S]}F_S(t_n+c_j\Delta t,u^{(j)}), \tag{6.9}$$

$$i=1,\cdots,s,$$

$$u_{n+1}=u_n+\Delta t\sum_{j=0}^{s}b_j^{[N]}F_N(t_n+c_j\Delta t,u^{(j)})+\Delta t\sum_{j=0}^{s}b_j^{[S]}F_S(t_n+c_j\Delta t,u^{(j)}), \tag{6.10}$$

where $u^{(0)}=u_n$ and $u^{(i)}$ approximates $u(t_n+c_i\Delta t)$. The non-stiff and stiff terms are integrated by their own $(s+1)$-stage Runge-Kutta methods respectively. The Butcher coefficients $a_{ij}^{[N]}$, $a_{ij}^{(S)}$, $b_j^{(N)}$, $b_j^{(S)}$ and c_j are constrained by order of accuracy and stability considerations. In [65], the implicit-explicit additive Runge-Kutta (ARK) methods from third- to fifth-order are presented in which the stiff terms are integrated by an L-stable, stiffly-accurate, singly diagonally implicit Runge-Kutta method while the non-stiff terms are integrated with a traditional explicit Runge-Kutta method. For a detailed description of the methods as well as their implementation and applications, we refer the readers to [65].

6.3 Exponential time differencing (ETD) methods

The ETD method was constructed to solve the equation of the following form

$$u_t=\mathcal{L}u+\mathcal{F}(t,u), \tag{6.11}$$

where $\mathcal{L}$ is a linear term and $\mathcal{F}$ is nonlinear. Many interesting equations are of this form, where typically $\mathcal{L}$ represents the stiff part of the equation. When discretizing in space we obtain a system of ODEs of the form

$$u_t = Lu + F(t,u). \tag{6.12}$$

The exponential time differencing (ETD) methods can be described in the context of solving (6.12). Integrating the equation over a single time step from $t=t_n$ to $t_{n+1}=t_n+\Delta t$, we get

$$u(t_{n+1}) = e^{L\Delta t}u(t_n) + e^{L\Delta t}\int_0^{\Delta t} e^{-L\tau}F(t_n+\tau,u(t_n+\tau))d\tau. \tag{6.13}$$

The equation (6.13) is exact. We denote the numerical approximation to $u(t_n)$ by u_n and write $F(t_n,u_n)$ as F_n. The simplest approximation to the integral (6.13) is to take F as a constant, $F = F_n + \mathcal{O}(\Delta t)$, on the interval $t_n \le t \le t_{n+1}$. Then we obtain the first order scheme ETD1, given by

$$u_{n+1} = e^{L\Delta t}u_n + L^{-1}(e^{L\Delta t} - I)F_n. \tag{6.14}$$

If instead of assuming that F is constant over the interval $t_n \le t \le t_{n+1}$, we use the linear approximation that

$$F = F_n + t(F_n - F_{n-1})/\Delta t + \mathcal{O}(\Delta t^2). \tag{6.15}$$

Then we obtain the second order scheme ETD2, given by

$$\begin{aligned} u_{n+1} =& e^{L\Delta t}u_n + \frac{1}{\Delta t}L^{-2}((I+\Delta tL)e^{L\Delta t} - I - 2\Delta tL)F_n \\ &+ \frac{1}{\Delta t}L^{-2}(-e^{L\Delta t} + I + \Delta tL)F_{n-1}. \end{aligned} \tag{6.16}$$

A second order ETD method of Runge-Kutta type, analogous to the ETD2 method, is as follows. First, the ETD1 (6.14) is taken to give

$$a_n = e^{L\Delta t}u_n + L^{-1}(e^{L\Delta t} - I)F_n. \tag{6.17}$$

Then the approximation

$$F = F(t_n,u_n) + (t-t_n)(F(t_n+\Delta t,a_n) - F(t_n,u_n))/\Delta t + \mathcal{O}(\Delta t^2), \tag{6.18}$$

is applied on the interval $t_n \le t \le t_{n+1}$, and is substituted into (6.13) to yield the scheme ETD2RK given by

$$u_{n+1} = a_n + \frac{1}{\Delta t}L^{-2}(e^{L\Delta t} - I - \Delta tL)(F(t_n+\Delta t,a_n) - F_n). \tag{6.19}$$

Cox and Matthews derive a set of ETD methods based on Runge-Kutta time-stepping, which they call ETDRK schemes in [43], among general formulas for ETD-schemes to arbitrary order. In a recent paper Kassam and Trefethen [64] compare various fourth order methods for solving equations of the form (6.12), and conclude that the best by a clear margin is a modification to the ETDRK schemes. In essence, for nonlinear time dependent equations, the ETD schemes provide a systematic coupling of the explicit treatment of nonlinearities and the implicit and possibly exact integration of the stiff linear parts of the equations, while achieving high accuracy and maintaining stability.

To overcome the vulnerability of the error cancelations in the high order ETD and ETDRK schemes, and to generalize the ETD schemes to non-diagonal problems, in [64], modified ETD schemes are proposed by using the complex contour integrals

$$f(L)=\frac{1}{2\pi i}\int_{\Gamma} f(z)(zI-L)^{-1}dz, \tag{6.20}$$

on a suitable contour Γ to evaluate the coefficients (e.g. $f(L)=L^{-2}(e^{L\Delta t}-I-\Delta tL)$ in (6.19)) in the update formula for ETDRK.

7 Concluding remarks and ongoing work

We have given a review on the algorithm design, analysis, implementation and application of LDG schemes for solving high order time-dependent PDEs. The extensive list of applications mentioned in this paper, or contained in the references and their references therein, would hopefully convince the readers the wide applicability of LDG schemes. We mention in this last section a few topics which are currently being investigated about LDG and in general about DG schemes:

Adaptivity

Adaptive methods are becoming exceedingly important in applications. The DG methods are ideally suited for adaptivity and parallelizability and might be the methods of choice for the use of adaptive strategies combined with load balancing techniques, not only in computational fluid dynamics but in a wide variety of problems of practical interest in mathematical physics. The LDG methods are flexible for general geometry, unstructured meshes and *h-p* adaptivity, and have high parallel efficiency. In order to be able to perform adaptivity while maintaining the high parallelizability of the DG methods, new high-order accurate time-stepping methods would have to be created which could use different time steps at different locations. We seek methods where h- and/or p-refinement may be performed on any element at any time. The benefit of the DG method is that the adaptive procedure only using local operations to alter element sizes or polynomial degrees. This is helpful to increase the accuracy and efficiency. The following issues should be considered in designing the adaptive strategy

- p-refinement;
- h-refinement;
- enrichment strategy.

It would be interesting to develop a scheme with the flexibility and high order accuracy but tailored specifically to the solution of nonlinear wave problems exhibiting highly localized dynamics. Such schemes have the potential to reduce the computation cost significantly.

Error estimate analysis

It is advantageous to know how to locally refine the mesh in order to obtain a better approximation. Estimates of discretization errors are essential to appraise solution accuracy and are, at the least, desirable to guide and control adaptive enrichment. A posteriori error estimation will be the first preparation for adaptive algorithms. How to design an error estimator applicable to a variety of nonlinear wave problems is the most important part in adaptive computation. As mentioned in [53], ideal a posteriori error estimates should be

- inexpensive relative to the cost of the solution;
- accurate in the sense that they converge to the true error under h- and p-refinement;
- robust in the sense that they provide error bounds over a wide range of mesh spacings, polynomial degrees, and norms.

Although there are some works [2,8,28,59,66,76,86,87] on error estimates for hyperbolic conservation law and parabolic problems, there are only a few works in the literature for error estimates of the LDG method for nonlinear wave equations with high order derivatives. It is more challenging to perform error estimates for nonlinear PDEs with high order derivatives than for first and second order PDEs.

Efficient and robust implicit time discretization

This would be helpful for situations with high order derivatives, or in an adaptive environment where the grid size might be very small in some regions. In order to be able to perform adaptivity while maintaining the high parallelizability of the DG methods, new high-order accurate time-stepping methods would have to be created which could use different time steps at different locations. The difficulty here is the high level of nonlinearity. For a fully implicit discretization, the resulting nonlinear system at each iteration is costly to solve, and certain iterative procedures such as the Newton's method does not seem to be robust. Exploring efficient linear and nonlinear solvers for discretizing LDG schemes for multi-dimensional problems with possible nonlinear higher order spatial derivative terms will be important issues.

Accuracy enhancement by post-processing

It is advantageous to know how to locally post-process the approximate solution in order to obtain a better approximation; this is particularly true in the framework of a posteriori error estimation and adaptive algorithms. For DG methods, this has been done, so far, in two different ways: by finding super-convergence points and by a local convolution. A post-processing accuracy enhancement technique developed by Cockburn, Luskin, Shu and Süli [36] is also applied to the numerical solutions of the KdV type equations by Yan and Shu [105]. The accuracy is enhanced from $(k+1)$-th order in L^2 norm to $(2k+1)$-th order in negative norm when P^k elements are used, indicating that a higher order of accuracy in negative-order norms is retained by all these methods. The applications of DG post-processing the approximate solution to other situations like wave propagation phenomena in general are also among our planned research at the next stage.

Acknowledgments

The research of the first author is support by NSFC grant 10601055, FANEDD of CAS and SRF for ROCS SEM. The research of the second author is supported by NSF grant DMS-0809086 and DOE grant DE-FG02-08ER25863.

References

[1] S. Adjerid and H. Temimi. A discontinuous Galerkin method for higher-order ordinary differential equations. Comput. Meth. Appl. Mech. Eng., 197:202–218, 2007.
[2] M. Ainsworth and J. Oden. A Posteriori Error Estimation in Finite Element Analysis, Computational and Applied Mathematics. Elsevier, 1996.
[3] V. Aizinger and C. Dawson. The local discontinuous Galerkin method for three-dimensional shallow water flow. Comput. Methods Appl. Mech. Engrg., 196:734–746, 2007.
[4] V. Aizinger, C. Dawson, B. Cockburn, and P. Castillo. The local discontinuous Galerkin method for contaminant transport. Advances in Water Resources, 24:73–87, 2000.
[5] A. Araújo, A. Murua, and J. Sanz-Serna. Symplectic methods based on decomposition. SIAM J. Numer. Anal., 34:1926–1947, 1997.
[6] D. N. Arnold. An interior penalty finite element method with discontinuous elements. SIAM J. Numer. Anal., 19:742–760, 1982.
[7] D. N. Arnold, F. Brezzi, B. Cockburn, and L. Marini. Unified analysis of discontinuous Galerkin methods for elliptic problems. SIAM J. Numer. Anal., 39:1749–1779, 2002.
[8] I. Babuška and T. Strouboulis. The Finite Element Method and its Reliability. Oxford University Press, 1999.
[9] G. Baker. Finite element methods for elliptic equations using nonconforming elements. Math. Comp., 31:45–59, 1977.
[10] F. Bassi and S. Rebay. A high-order accurate discontinuous finite element method for the numerical solution of the compressible Navier-Stokes equations. J. Comput. Phys., 131:267–279, 1997.

[11] C. Baumann and J. Oden. A discontinuous *hp* finite element method for convection-diffusion problems. Comput. Meth. Appl. Mech. Eng., 175:311–341, 1999.
[12] R. Biswas, K. Devine, and J. Flaherty. Parallel, adaptive finite element methods for conservation laws. Appl. Numer. Math., 14:255–283, 1994.
[13] E. Burman and B. Stamm. Local discontinuous Galerkin method with reduced stabilization for diffusion equations. Commun. Comput. Phys., 5:498–514, 2009.
[14] R. Bustinza. A unified analysis of the local discontinuous Galerkin method for a class of nonlinear problems. Appl. Numer. Math., 56:1293–1306, 2006.
[15] R. Bustinza and G. Gatica. A local discontinuous Galerkin method for nonlinear diffusion problems with mixed boundary conditions. SIAM J. Sci. Comput., 26:152–177, 2004.
[16] R. Bustinza and G. Gatica. A local discontinuous Galerkin method for nonlinear diffusion problems with mixed boundary conditions. J. Comput. Phys., 207:427–456, 2005.
[17] R. Bustinza, G. Gatica, and B. Cockburn. An A posteriori error estimate for the local discontinuous Galerkin method applied to linear and nonlinear diffusion problems. J. Sci. Comput., 22-23:147–185, 2005.
[18] R. Bustinza, G. Gatica, and F. Sayas. On the coupling of local discontinuous Galerkin and boundary element methods for non-linear exterior transmission problems. IMA J. Numer. Anal., 28:225–244, 2008.
[19] P. Castillo. An a posteriori error estimate for the local discontinuous Galerkin method. J. Sci. Comput., 22-23:187–204, 2005.
[20] P. Castillo. A review of the Local Discontinuous Galerkin (LDG) method applied to elliptic problems. Appl. Numer. Math., 56:1307–1313, 2006.
[21] P. Castillo, B. Cockburn, I. Perugia, and D. Schotzau. An a priori error analysis of the local discontinuous Galerkin method for elliptic problems. SIAM J. Numer. Anal., 38:1676–1706, 2000.
[22] P. Castillo, B. Cockburn, I. Perugia, and D. Schotzau. Local discontinuous Galerkin methods for elliptic problems. Communications in Numerical Methods in Engineering, 18:69–75, 2002.
[23] P. Castillo and E. Velazquez. A numerical study of a semi-algebraic multilevel preconditioner for the local discontinuous Galerkin method. Int. J. Numer. Methods Eng., 74:255–268, 2008.
[24] H. Chen. Pointwise error estimates of the local discontinuous Galerkin method for a second order elliptic problem. Math. Comp., 74:1097–1116, 2005.
[25] Y. Cheng and C.-W. Shu. A discontinuous Galerkin finite element method for time dependent partial differential equations with higher order derivatives. Math. Comp., 77:699–730, 2008.
[26] B. Cockburn. Discontinuous Galerkin methods for convection-dominated problems. In T. Barth and H. Deconinck, editors, High-Order Methods for Computational Physics, volume 9 of Lecture Notes in Computational Science and Engineering, pages 69–224. Springer, Berlin, 1999.
[27] B. Cockburn and B. Dong. An analysis of the minimal dissipation local discontinuous Galerkin method for convection-diffusion problems. J. Sci. Comput., 32:233–262, 2007.
[28] B. Cockburn and P. Gremaud. Error estimates for finite element methods for nonlinear conservation laws. SIAM J. Numer. Anal., 33:522–554, 1996.
[29] B. Cockburn, S. Hou, and C.-W. Shu. The Runge-Kutta local projection discontinuous Galerkin finite element method for conservation laws IV: the multidimensional case. Math. Comp., 54:545–581, 1990.

[30] B. Cockburn, G. Kanschat, and D. Schotzau. The local discontinuous Galerkin method for the Oseen equations. Math. Comp., 73:569–593, 2004.
[31] B. Cockburn, G. Kanschat, and D. Schotzau. A locally conservative LDG method for the incompressible Navier-Stokes equations. Math. Comp., 74:1067–1095, 2005.
[32] B. Cockburn, G. Kanschat, and D. Schotzau. The local discontinuous Galerkin method for linearized incompressible fluid flow: a review. Comput. & Fluids, 34:491–506, 2005.
[33] B. Cockburn, G. Kanschat, D. Schotzau, and C. Schwab. Local discontinuous Galerkin methods for the Stokes system. SIAM J. Numer. Anal., 40:319–343, 2002.
[34] B. Cockburn, G. Karniadakis, and C.-W. Shu. The development of discontinuous Galerkin methods. In B. Cockburn, G. Karniadakis, and C.-W. Shu, editors, Discontinuous Galerkin Methods: Theory, Computation and Applications, volume 11 of Lecture Notes in Computational Science and Engineering, pages 3–50. Springer, Berlin, 2000.
[35] B. Cockburn, S.-Y. Lin, and C.-W. Shu. TVB Runge-Kutta local projection discontinuous Galerkin finite element method for conservation laws III: one dimensional systems. J. Comput. Phys., 84:90–113, 1989.
[36] B. Cockburn, M. Luskin, C.-W. Shu, and E. Süli. Enhanced accuracy by post-processing for finite element methods for hyperbolic equations. Math. Comp., 72:577–606, 2003.
[37] B. Cockburn and C.-W. Shu. TVB Runge-Kutta local projection discontinuous Galerkin finite element method for conservation laws II: general framework. Math. Comp., 52:411–435, 1989.
[38] B. Cockburn and C.-W. Shu. The local discontinuous Galerkin method for time-dependent convection-diffusion systems. SIAM J. Numer. Anal., 35:2440–2463, 1998.
[39] B. Cockburn and C.-W. Shu. The Runge-Kutta discontinuous Galerkin method for conservation laws V: multidimensional systems. J. Comput. Phys., 141:199–224, 1998.
[40] B. Cockburn and C.-W. Shu. Runge-Kutta discontinuous Galerkin methods for convection-dominated problems. J. Sci. Comput., 16:173–261, 2001.
[41] B. Cockburn and C.-W. Shu. Foreword for the special issue on discontinuous Galerkin method. J. Sci. Comput., 22-23:1–3, 2005.
[42] B. Cockburn and C.-W. Shu. Foreword for the special issue on discontinuous Galerkin method. J. Sci. Comput., 40:1–3, 2009.
[43] S. Cox and P. Matthews. Exponential time differencing for stiff systems. J. Comput. Phys., 176:430–455, 2002.
[44] C. Dawson. The P^{k+1} S^k local discontinuous Galerkin method for elliptic equations. SIAM J. Numer. Anal., 40:2151–2170, 2003.
[45] C. Dawson. Coupling local discontinuous and continuous Galerkin methods for flow problems. Advances in Water Resources, 28:729–744, 2005.
[46] C. Dawson. Foreword for the special issue on discontinuous Galerkin method. Comput. Meth. Appl. Mech. Engin., 195:3183, 2006.
[47] C. Dawson and J. Proft. A priori error estimates for interior penalty versions of the local discontinuous Galerkin method applied to transport equations. Numerical Methods for Partial Differential Equations, 17:545–564, 2001.
[48] B. Dong and C.-W. Shu. Analysis of a local discontinuous Galerkin method for fourth-order time-dependent problems. SIAM J. Numer. Anal. submitted.
[49] A. Dutt, L. Greengard, and V. Rokhlin. Spectral deferred correction methods for ordinary differential equations. BIT, 40:241–266, 2000.
[50] C. Eskilsson and S. Sherwin. A discontinuous spectral element model for Boussinesq-type equations. J. Sci. Comput., 17:143–152, 2002.

[51] C. Eskilsson and S. Sherwin. Discontinuous Galerkin spectral/hp element modelling of dispersive shallow water systems. J. Sci. Comput., 22/23:269–288, 2005.
[52] C. Eskilsson and S. Sherwin. Spectral/hp discontinuous Galerkin methods for modelling 2D Boussinesq equations. J. Comput. Phys., 212:566–589, 2006.
[53] J. E. Flaherty, L. Krivodonova, J.-F. Remacle, and M. S. Shephard. Aspects of discontinuous Galerkin methods for hyperbolic conservation laws. Finite Elem. Anal. Des., 38:889–908, 2002.
[54] G. Gassner, F. Lörcher, and C.-D. Munz. A contribution to the construction of diffusion fluxes for finite volume and discontinuous Galerkin schemes. J. Comput. Phys., 224:1049–1063, 2007.
[55] S. Gottlieb and C.-W. Shu. Total variation diminishing Runge-Kutta schemes. Math. Comp., 67:73–85, 1998.
[56] J. Guzmán and B. Rivière. Sub-optimal convergence of non-symmetric discontinuous Galerkin methods for odd polynomial approximations. J. Sci. Comput., 40:273–280, 2009.
[57] J. Haink and C. Rohde. Local discontinuous-Galerkin schemes for model problems in phase transition theory. Commun. Comput. Phys., 4:860–893, 2008.
[58] J. Hesthaven and T. Warburton. Nodal Discontinuous Galerkin Methods. Springer, New York, 2008.
[59] P. Houston, E. Süli, and C. Schwab. Stabilized hp-finite element methods for hyperbolic problems. SIAM J. Numer. Anal., 37:1618–1643, 2001.
[60] G. Jiang and C.-W. Shu. On a cell entropy inequality for discontinuous Galerkin methods. Math. Comp., 62:531–538, 1994.
[61] G. Kanschat. Preconditioning methods for local discontinuous Galerkin discretizations. SIAM J. Sci. Comput., 25:815–831, 2003.
[62] G. Kanschat. Block preconditioners for LDG discretizations of linear incompressible flow problems. J. Sci. Comput., 22-23:371–384, 2005.
[63] G. Kanschat. Discontinuous Galerkin Methods for Viscous Flow. Deutscher Universitätsverlag, Wiesbaden, 2007.
[64] A.-K. Kassam and L. Trefethen. Fourth-order time stepping for stiff problem. SIAM J. Sci. Comput., 26:1214–1233, 2005.
[65] C. Kennedy and M. Carpenter. Additive Runge-Kutta schemes for convection-diffusion-reaction equations. Appl. Num. Math., 44:139–181, 2003.
[66] M. Larson and T. Barth. A posteriori error estimation for discontinuous Galerkin approximations of hyperbolic systems. In B. Cockburn, G. Karniadakis, and C.-W. Shu, editors, Discontinuous Galerkin Methods: Theory, Computation and Applications, volume 11 of Lecture Notes in Computational Science and Engineering, pages 221–230. Springer, 2000.
[67] D. Levy, C.-W. Shu, and J. Yan. Local discontinuous Galerkin methods for nonlinear dispersive equations. J. Comput. Phys., 196:751–772, 2004.
[68] B. Li. Discontinuous Finite Elements in Fluid Dynamics and Heat Transfer. Birkhauser, Basel, 2006.
[69] H. Li, M. Farthing, C. Dawson, and C. Miller. Local discontinuous Galerkin approximations to Richards' equation. Advances in Water Resources, 30:555–575, 2007.
[70] H. Li, M. Farthing, and C. Miller. Adaptive local discontinuous Galerkin approximation to Richards' equation. Advances in Water Resources, 30:1883–1901, 2007.
[71] H. Liu and J. Yan. A local discontinuous Galerkin method for the KdV equation with boundary effect. J. Comput. Phys., 215:197–218, 2006.
[72] H. Liu and J. Yan. The Direct Discontinuous Galerkin (DDG) methods for diffusion prob-

lems. SIAM J. Numer. Anal., 47:675–698, 2008.
[73] T. Lu, W. Cai, and P. Zhang. Conservative local discontinuous Galerkin methods for time dependent Schrödinger equation. Int. J. Numer. Anal. Model., 2:75–84, 2005.
[74] M. Minion. Semi-implicit spectral deferred correction methods for ordinary differential equations. Commun. Math. Sci., 1:471–500, 2003.
[75] J. Oden, I. Babuvska, and C. Baumann. A discontinuous hp finite element method for diffusion problems. J. Comput. Phys., 146:491–519, 1998.
[76] N. Pierce and M. Giles. Adjoint recovery of superconvergent functionals from PDE approximation. SIAM Review, 42:247–264, 2000.
[77] W. Reed and T. Hill. Triangular mesh methods for the neutrontransport equation. La-ur-73-479, Los Alamos Scientific Laboratory, 1973.
[78] J.-F. Remacle, J. Flaherty, and M. Shephard. An adaptive discontinuous Galerkin technique with an orthogonal basis applied to Rayleigh-Taylor ow instabilities. SIAM Rev., 45:53–72, 2003.
[79] B. Rivière. Discontinuous Galerkin methods for solving elliptic and parabolic equations. Theory and implementation. SIAM, 2008.
[80] P. Rosenau and J. Hyman. Compacton: Solitons with finite wavelength. Phys. Rev. Lett., 70:564–567, 1993.
[81] D. Schotzau. Local discontinuous Galerkin methods for incompressible flow. Computational Fluid and Solid Mechanics, 1-2:1116–1118, 2003.
[82] C.-W. Shu. TVB uniformly high-order schemes for conservation laws. Math. Comp, 49:105–121, 1987.
[83] C.-W. Shu. Different formulations of the discontinuous Galerkin method for the viscous terms. In Z.-C. Shi, M. Mu, W. Xue, and J. Zou, editors, Advances in Scientific Computing, pages 144–155. Science Press, Beijing, 2001.
[84] C.-W. Shu. Discontinuous Galerkin methods: general approach and stability. In S. Bertoluzza, S. Falletta, G. Russo, and C.-W. Shu, editors, Numerical Solutions of Partial Differential Equations, pages 149–201. Birkhäuser, Basel, 2009.
[85] C.-W. Shu and S. Osher. Efficient implementation of essentially non-oscillatory shock-capturing schemes. J. Comput. Phys., 77:439–471, 1988.
[86] E. Süli. A posteriori error analysis and adaptivity for finite element approximations of hyperbolic problems. In D. Kroner, M. Ohlberger, and C. Rhode, editors, An Introduction to Recent Developments in Theory and Numerics for Conservation Laws, volume 5 of Lecture Notes in Computational Science and Engineering, pages 123–194. Springer, 1999.
[87] E. Süli, C. Schwab, and P. Houston. Hp-DGFEM for partial differential equations with non-negative characteristic form. In B. Cockburn, G. Karniadakis, and C.-W. Shu, editors, Discontinuous Galerkin Methods: Theory, Computation and Applications, volume 11 of Lecture Notes in Computational Science and Engineering, pages 221–230. Springer, 2000.
[88] B. van Leer and S. Nomura. Discontinuous Galerkin for diffusion. Proceedings of 17th AIAA Computational Fluid Dynamics Conference (June 6-9 2005) , 2005. AIAA-2005-5108.
[89] M. van Raalte and B. van Leer. Bilinear forms for the recovery-based discontinuous Galerkin method for diffusion. Commun. Comput. Phys., 5:683–693, 2009.
[90] E. Velazquez and P. Castillo. An adaptive strategy for the local discontinuous Galerkin method applied to porous media problems. Computer-Aided Civil and Infrastructure Engineering, 23:238–252, 2008.
[91] W. Wang and C.-W. Shu. The WKB local discontinuous Galerkin method for the simulation of Schrödinger equation in a resonant tunneling diode. J. Sci. Comput., 40:360–374, 2009.

[92] Y. Xia, Y. Xu, and C.-W. Shu. Efficient time discretization for local discontinuous Galerkin methods. Discrete Contin. Dyn. Syst. Ser. B, 8:677–693, 2007.
[93] Y. Xia, Y. Xu, and C.-W. Shu. Local discontinuous Galerkin methods for the Cahn-Hilliard type equations. J. Comput. Phys., 227:472–491, 2007.
[94] Y. Xia, Y. Xu, and C.-W. Shu. Application of the local discontinuous Galerkin method for the Allen-Cahn/Cahn-Hilliard system. Commun. Comput. Phys., 5:821–835, 2009.
[95] Z. Xie, Z. Zhang, and Z. Zhang. A numerical study of uniform superconvergence of LDG method for solving singularly perturbed problems. J. Comput. Math., 27:280–298, 2009.
[96] Y. Xu and C.-W. Shu. Local discontinuous galerkin methods for three classes of nonlinear wave equations. J. Comput. Math., 22:250–274, 2004.
[97] Y. Xu and C.-W. Shu. Local discontinuous Galerkin methods for nonlinear Schrödinger equations. J. Comput. Phys., 205:72–97, 2005.
[98] Y. Xu and C.-W. Shu. Local discontinuous Galerkin methods for two classes of two dimensional nonlinear wave equations. Physica D, 208:21–58, 2005.
[99] Y. Xu and C.-W. Shu. Local discontinuous Galerkin methods for the Kuramoto-Sivashinsky equations and the Ito-type coupled KdV equations. Comput. Methods Appl. Mech. Engrg., 195:3430–3447, 2006.
[100] Y. Xu and C.-W. Shu. Error estimates of the semi-discrete local discontinuous Galerkin method for nonlinear convection-diffusion and KdV equations. Comput. Methods Appl. Mech. Engrg., 196:3805–3822, 2007.
[101] Y. Xu and C.-W. Shu. A local discontinuous Galerkin method for the Camassa-Holm equation. SIAM J. Numer. Anal., 46:1998–2021, 2008.
[102] Y. Xu and C.-W. Shu. Local discontinuous Galerkin method for the Hunter-Saxton equation and its zero-viscosity and zero-dispersion limit. SIAM J. Sci. Comput., 31:1249–1268, 2008.
[103] Y. Xu and C.-W. Shu. Local discontinuous Galerkin method for surface diffusion and Willmore flow of graphs. J. Sci. Comput., 40:375–390, 2009.
[104] J. Yan and C.-W. Shu. A local discontinuous Galerkin method for KdV type equations. SIAM J. Numer. Anal., 40:769–791, 2002.
[105] J. Yan and C.-W. Shu. Local discontinuous Galerkin methods for partial differential equations with higher order derivatives. J. Sci. Comput., 17:27–47, 2002.
[106] L. Yuan and C.-W. Shu. Discontinuous Galerkin method based on non-polynomial approximation spaces. J. Comput. Phys., 218:295–323, 2006.
[107] L. Yuan and C.-W. Shu. Discontinuous Galerkin method for a class of elliptic multi-scale problems. Internat. J. Numer. Methods Fluids, 56:1017–1032, 2008.
[108] M. Zhang and C.-W. Shu. An analysis of three different formulations of the discontinuous Galerkin method for diffusion equations. Math. Models Methods Appl. Sci., 13:395–413, 2003.
[109] Q. Zhang and Z. Wu. Numerical simulation for porous medium equation by local discontinuous Galerkin finite element method. J. Sci. Comput., 38:127–148, 2009.